Journal of Controlled Release 366 (2024) 650–667

Contents lists available at ScienceDirect

Journal of Controlled Release

journal homepage: www.elsevier.com/locate/jconrel

Review article

Electromechanical convective drug delivery devices for overcoming diffusion barriers

Jihoon Park [a], Ramy Ghanim [a], Adwik Rahematpura [b], Caroline Gerage [a], Alex Abramson [a,b,c,*]

[a] School of Chemical and Biomolecular Engineering, Georgia Institute of Technology, Atlanta, GA 30332, USA
[b] The Wallace H. Coulter Department of Biomedical Engineering, Georgia Institute of Technology, Atlanta, GA 30332, USA
[c] Division of Digestive Diseases, Emory University School of Medicine, Atlanta, GA 30322, USA

ARTICLE INFO

Keywords:
Convective drug delivery
Robotic devices
Tissue barriers
Synergies of diffusive and convective drug delivery

ABSTRACT

Drug delivery systems which rely on diffusion for mass transport, such as hydrogels and nanoparticles, have enhanced drug targeting and extended delivery profiles to improve health outcomes for patients suffering from diseases including cancer and diabetes. However, diffusion-dependent systems often fail to provide >0.01–1% drug bioavailability when transporting macromolecules across poorly permeable physiological tissues such as the skin, solid tumors, the blood-brain barrier, and the gastrointestinal walls. Convection-enabling robotic ingestibles, wearables, and implantables physically interact with tissue walls to improve bioavailability in these settings by multiple orders of magnitude through convective mass transfer, the process of moving drug molecules via bulk fluid flow. In this Review, we compare diffusive and convective drug delivery systems, highlight engineering techniques that enhance the efficacy of convective devices, and provide examples of synergies between the two methods of drug transport.

1. Introduction

Diffusion-based drug delivery systems passively elute therapeutics from a high concentration formulation, such as a hydrogel, into a lower concentration environment. These biomaterials provide patients with therapies that enable: tunable sustained release profiles that reduce dosing frequencies; cell targeting capabilities that reduce off-target side effects; and high biocompatibilities that mitigate the foreign body response [1–3]. However, controlled release and nanomedicine formulations suffer significant hurdles during clinical translation. The disconnect between the vast number of academic papers and few clinical approvals by the US Food and Drug Administration (FDA) for nanoparticles and hydrogels has generated questions about the utility of these technologies [4,5]. When biomacromolecular drugs need to diffuse across a poorly permeable physiological barrier, their bioavailabilities fall to 1% or less [6–9]. For example, around 0.7% of nanoparticles reach tumors after intravenous injections [7], while the bioavailabilities of orally, intragastrically, topically, and intranasally administered peptides are approximately 1% [8], <0.1% [10], <0.1% [11], and 1–3% [6,9], respectively. Strategies to facilitate transport across physiological diffusion barriers, such as loosening tight junctions [12,13], exploiting receptor mediated transcellular transport [14–17], ionic liquids [18–20], protease inhibitors [21], and permeation enhancers [22,23] have been developed, but modest diffusion coefficient improvements still keep bioavailabilities in the low single digits. Especially for drugs with injection doses over 1 mg/week, the monetary and volume constraints associated with loading 100 times as much drug hold these alternative delivery technologies back from clinical translation [24,25]. Additional complications such as initial burst releases, lack of control over spatiotemporal concentration profiles, and inability to make modifications following administration remain key challenges in the field.

To overcome the limitations of diffusion-based formulations, convection-based delivery systems transfer drugs via bulk fluid flow. This allows macromolecules to travel further into tissue, in part by physically disrupting diffusion barriers and also by utilizing pressure gradients to push formulations into narrow crevasses. In 1994, Oldfield's group developed a novel method for drug delivery in the brain called convection-enhanced delivery (CED) [26]. By inserting catheters directly into the brain, they delivered an infusion of low and high molecular weight compounds, sucrose (359 Da) and transferrin (80 kDa), to a large volume of the brain. Immediately after two-hour infusions, sucrose and transferrin spread approximately 2 cm and 1.5 cm from their initial locations, respectively; if these molecules were distributed solely

* Corresponding author at: School of Chemical and Biomolecular Engineering, Georgia Institute of Technology, Atlanta, GA 30332, USA.
E-mail address: aabramson6@gatech.edu (A. Abramson).

https://doi.org/10.1016/j.jconrel.2024.01.008
Received 8 September 2023; Received in revised form 2 January 2024; Accepted 3 January 2024
Available online 17 January 2024

by diffusion, the estimated average depths of tissue penetration are only 0.39 cm and 0.07 cm, respectively. Convection enhances the depth of tissue penetration by multiple orders of magnitude, with the effect being magnified for larger molecules. In addition to enhanced distribution profiles and bioavailabilities, convection-based systems can also actively regulate drug release timings, granting greater control over the drug's spatiotemporal concentration profile [26,27]. However, developing convection-based methods requires engineering complex, invasive, and expensive electromechanical devices that localize to the targeted tissue area and insert drug into the appropriate tissue layer. For this reason, convective devices are only recently reaching the clinic.

In this Review, we describe the challenges behind engineering convection-enabling drug delivery devices, quantify the advantages these systems have over diffusion-based delivery, and highlight tissues that benefit from convection-based methods. First, we analyze mass transport models estimating tissue penetration depths of macromolecules by diffusion and convection. We describe the length scales of various physiological barriers in the body and the timescales required for macromolecules to diffuse across those barriers. Based on the models and barriers, we then discuss the clinical successes and failures of diffusion-based methods. Next, we introduce convection-enabling devices that enhance drug delivery across barriers to enable unique targeting and release profiles. We then compare these systems to devices that physically disrupt tissue barriers but still rely on diffusion for mass transport, and we show that convective systems provide superior drug distribution over these other technologies. Finally, we highlight engineering techniques to obtain optimal drug distribution patterns by convective drug delivery. Through this analysis, we provide insight into how convective systems could augment the field of drug delivery to achieve more efficient and controlled release profiles to areas of the body where diffusion-based transport alone does not yield sufficient therapeutic efficacy.

2. Mass transport models

In this section, we compare various properties of diffusion-based and convection-based methods, including mathematical models developed to analyze mass transport, typical drug penetration depths, and resulting drug concentration profiles (Fig. 1).

2.1. Diffusion-based methods

Diffusion is a mode of mass transport achieved by random motion of molecules due to thermal energy. For Fickian diffusion, the diffusive mass flux (J_D) is expressed as the negative of the product of the diffusion coefficient (D) and the concentration gradient (∇C):

$$J_D = -D\nabla C \tag{1}$$

The diffusion coefficient is an indicator of the rate of diffusion of each molecule. For spherical molecules under creeping flow, its value

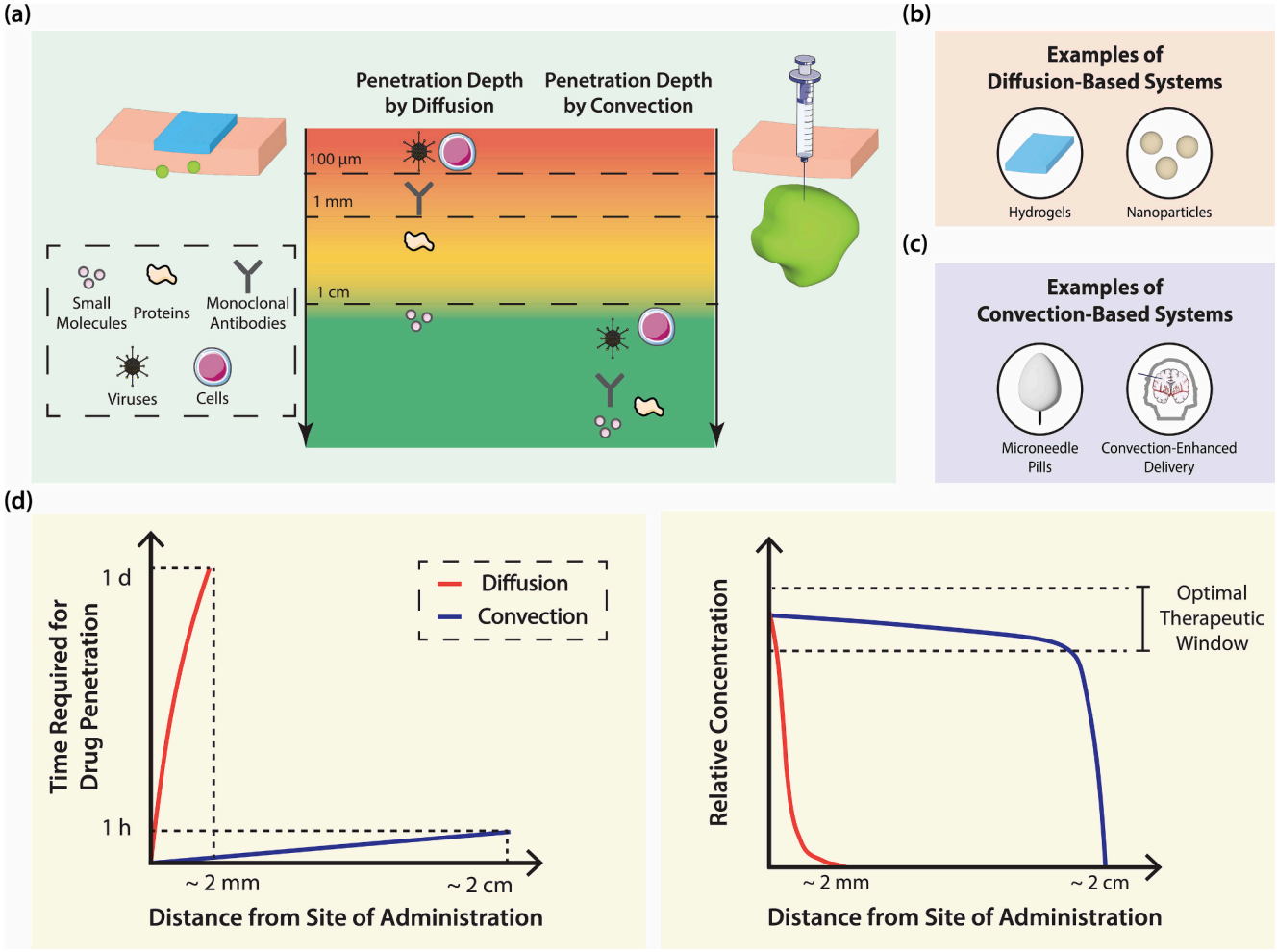

Fig. 1. Overview of diffusion-based and convection-based drug delivery systems. (a) The orders of magnitude of tissue penetration depths of commonly administered drugs are compared. Examples of (b) diffusion-based and (c) convection-based drug delivery systems are illustrated. (d) Time required for drug penetration and resulting drug concentration profiles. Parts of the figure were adapted from Servier Medical Art, CC BY license.

(D_0) can be estimated with the Stokes-Einstein relation:

$$D_0 = \frac{kT}{6\pi\eta R} \tag{2}$$

where k is the Boltzmann constant, T is the absolute temperature, η is the viscosity of the solution, and R is the hydrodynamic radius of the molecule. Diffusion coefficients are typically smaller for molecules with greater hydrodynamic radii, as can be inferred from eq. 2.

For one dimensional diffusion, the average timescale (τ_D) required for molecules to diffuse over a given distance is proportional to the square of the distance $\left(l^2\right)$ and the inverse of the diffusion coefficient:

$$\tau_D = \frac{l^2}{2D} \tag{3}$$

As a result, diffusion is an efficient mode of mass transfer for small molecules or for macromolecules over short distances such as within a single cell, but macromolecular diffusion over long distances or through impermeable barriers is extremely time-consuming. For example, when purely transported by diffusion, it only requires approximately 1 h for an IgG molecule to diffuse through 100 μm in the interstitial space, while approximately 2 days are required to travel 1 mm [28]. In addition, especially for macromolecules, the extracellular matrix (ECM) hinders diffusion through tissue. Its components such as hyaluronic acid and collagen physically block the passage of macromolecules, increasing the tortuosity and path length. Molecular interactions such as hydrodynamic and steric interactions further impede the macromolecule penetration [29]. While the extent of hindrance depends on the specific molecule and tissue, generally the hindrance becomes more pronounced with larger molecules, resulting in diffusion coefficients that shrink by 1–2 orders of magnitude for every order of magnitude increase in molecular weight. In some cases, limited diffusivity can be beneficial, such as when minimizing extravasation of nanoparticles from blood vessels to target the lymph nodes [30]. However, when targeting specific tissues located in the inner regions of organs or behind diffusion barriers, the bulkiness of macromolecular drugs significantly delays or even prevents their distribution.

Poor macromolecular diffusivity presents a significant challenge when delivering drugs by diffusion across physiological barriers. For example, ingested drugs must diffuse across the mucus layer and tight junctions of the GI tract, and macromolecules targeted against tumors must first diffuse out of a formulated hydrogel and then across the interstitial space to reach the tumor core. Both mathematical modeling and in vivo studies illustrate that impractically steep concentration gradients (∇C), extremely long time scales, or both are required for drugs to penetrate through these barriers [26,31].

When healthcare professionals implant drug reservoirs to reach blood vessels for systemic delivery or diseased tissues in the inner regions of an organ, macromolecules must first diffuse through the tightly packed outermost layers of tissue designed to prevent diffusion of these exact molecules, such as the epithelial layers of the GI tract and the endothelial layers of the blood-brain barrier (BBB). Molecules diffuse across these barriers by either paracellular or transcellular diffusion [32]. Paracellular diffusion refers to diffusion across the tight junctions between epithelial or endothelial cells, by either the pore or leak pathways. The pore pathway is both size- and charge-selective; while the cutoff threshold may vary depending on the specific position, many pores exclude molecules larger than 5–10 Å [33,34], and are impermeable to macromolecules such as proteins. The leak pathway is more forgiving to larger molecules, but its capacity for macromolecular diffusion flux is limited [33,34]. Strategies such as loosening tight junctions are being developed [12,13], but concerns around increased flux of toxic and undesired molecules like pathogens and undigested food exist. The alternative, transcellular diffusion, is diffusion through the epithelial or endothelial cells [35]. Because the large size of macromolecules inhibits diffusion directly through the lipid bilayers, the only remaining method is to enter the cells by interacting with membrane proteins such as transporters, followed by exiting the cells in a similar fashion. While studies of exploiting interactions with various membrane proteins such as transferrin receptors [14], glucose transporters [15] and insulin receptors [16] of the BBB, as well as organic anion transporting polypeptide families [17] of the GI tract have been conducted, the efficiencies of these pathways are currently too low to be clinically translated [36]. Remaining macromolecules next must diffuse over the inner tissue layers to reach their target. For example, after crossing the BBB, drugs must reach glioblastomas. While diffusion across these inner layers may be less tightly regulated compared to crossing tight junctions, the diffusion coefficients of macromolecules remain very small, on the order of 10^{-12}–10^{-11} m^2/s for proteins [37,38]. In addition, they must diffuse over much longer distances compared to endothelial and epithelial layers. For example, the stomach and the left ventricular free wall are thicker than 1 cm [39,40]. Thus, diffusion timescales required to pass through these layers become prohibitively long, especially in large animals. A hypothetical protein that diffuses out of a hydrogel on the epicardial surface of a human heart with a diffusion coefficient of 10^{-11} m^2/s would require several months to diffuse across the entire left ventricular free wall.

While intravenously administered particles are distributed via convection in the bloodstream, they too face diffusion hurdles. Prior to clearance, particles must extravasate from blood vessels to the target [41,42]. Upon entering the bloodstream, administered particles pass multiple organs, such as the liver, kidney, and spleen. The kidneys excrete particles smaller than 5.5 nm, while phagocytic cells, the liver, and the spleen clear larger particles [43,44]. In normal tissue, blood vessel walls do not leak, and larger particles cannot easily escape through the tight junctions between the endothelial cells of the blood vessels [45]. As a result, systemically administered macromolecules require large doses to reach therapeutically relevant concentrations. After extravasation, the particles must diffuse approximately 100 μm in the interstitial space to their target [45], as blood vessels are located approximately every 200 μm [28].

For diseases which require rapid distribution of drug such as diabetes and myocardial infarction, the slow distribution of molecules by diffusion can prevent a drug from reaching its therapeutic level in time; for example, the formation of fibrous capsules around soft devices secreting insulin halved the ability to moderate blood glucose levels after 3 weeks and further reduced the ability following 8 weeks of implantation [46]. In another study where scientists implanted hydrogel spheres encapsulating pancreatic islet cells secreting insulin in diabetic mice, fibrotic foreign body responses regularly led to treatment failure [47]. When they used large spheres, blood glucose levels remained at healthy levels for up to 180 days, whereas when they used small spheres, a severe foreign body response prevented glycemic control following just 5 weeks of implantation.

The delay in drug distribution can be less detrimental for chronic diseases dosed periodically, particularly when the dosing interval is similar to, or exceeds diffusion timescales. For example, Keytruda® and Remicade® are administered intravenously every three weeks to treat advanced melanomas and active psoriatic arthritis, respectively. However, when diffusion timescales are long – on the scales of days to weeks – other factors must be considered. Drugs may degrade in the bloodstream or interstitial space due to their inherent instability, cellular uptake, or degradation via extracellular enzymes. For example, endothelial cells continuously clear monoclonal antibodies in blood plasma [48,49]. Scientists utilize PEGylation to increase nanoparticles' circulation time, but the formation of anti-PEG antibodies and accelerated blood clearance upon repeated dosing can result in treatment failure [50]. In addition, if the target region is close to barriers lined with transporters, drugs can be cleared into the bloodstream at a rate greater than that they are eluted from their reservoirs or penetrate the barriers. Thus, the drugs may not be able to reach their target or will achieve a concentration too low to elicit a therapeutic response. For example,

drugs that enter the brain are eliminated rapidly into the bloodstream by the transporters of the BBB [51–53].

Another drawback of diffusion-based methods is their lack of control over the spatiotemporal concentration profile of released drugs. While release kinetics from diffusion-based methods such as hydrogels can be tuned, many show either: i) an initial burst release profile [1,54] which yields initially toxic drug levels before leveling out to concentrations within the pre-programmed therapeutic windows, or ii) a sustained release profile [1,2]. Obtaining complex release profiles with multiple burst releases requires complex manufacturing processes, and drug loading efficiency is reduced. McHugh and colleagues have developed nanoparticle-based drugs capable of multiple burst releases on μg-level doses [55,56], but systems capable of delivering mg-level doses are yet to be reported.

Finally, diffusion-dependent systems are pre-programmed. Once hydrogels or nanoparticles are administered, their release kinetics cannot be further tuned; no changes can be made to when or how fast their cargo is released. While diffusion-based methods can be engineered to release cargo at specific time points upon triggering by external stimuli such as through ultrasound [57] or infrared light [58], the resulting spatiotemporal concentration profile of drugs cannot be modified once administered. On the other hand, convection-based methods can deliver drugs rapidly across diffusion barriers while imparting more control over the resulting spatiotemporal concentration profile of drugs. In the next subsection, we discuss how convection-based methods overcome the limitations of diffusion-based methods.

2.2. Convection-based methods

Convective mass transport occurs when particles are transported by bulk fluid flow. At low flowrates, bulk fluid flow in tissues can be modeled using a modified form of Darcy's law [26,29,31]:

$$u = -\kappa \nabla p \tag{4}$$

where u is the interstitial velocity of the fluid, κ is the hydraulic conductivity of the tissue, and ∇p is the pressure gradient. The resulting convective mass flux J_c can be expressed as:

$$J_c = u \times R_{F,i} \times C_i = -\kappa C_i R_{F,i} \nabla p \tag{5}$$

where $R_{F,i}$ and C_i are the retardation factor and concentration of each species, respectively.

To compare the relative contributions of diffusion and convection to the mass transfer rate within the same medium, the Péclet number (Pe) is used:

$$\begin{aligned} \mathrm{Pe} &= \frac{\mathrm{u} \times \mathrm{l}}{\mathrm{D}} = \frac{\text{convective mass transfer rate}}{\text{diffusive mass transfer rate}} \\ &= \frac{\mathrm{l}^2/\mathrm{D}}{\mathrm{l}/\mathrm{u}} = \frac{\text{diffusion timescale}}{\text{convection timescale}} \end{aligned} \tag{6}$$

To compare the relative contributions of diffusion in the tissue and convection in the infusate, we replace the diffusion coefficient in the infusate with that within tissue. As an example, for the protein transferrin from Oldfield's initial demonstration of CED, we can estimate the ratio of relative mass transfer contributions by assuming a spherical, radially homogeneous injection profile and a diffusion coefficient of $10^{-11}\mathrm{m}^2/\mathrm{s}$ [26]:

$$\frac{\text{convective mass transfer rate}}{\text{diffusive mass transfer rate}} \approx \frac{1.5 \times 10^{-8\frac{\mathrm{m}}{\mathrm{s}}} \times 1.5 \times 10^{-2}\mathrm{m}}{10^{-11\frac{\mathrm{m}^2}{\mathrm{s}}}} = 22$$

While this ratio is an estimate, it clearly demonstrates that the contribution of diffusion for macromolecular distribution is negligible compared to that of convection. In tissues other than the brain where greater flowrates and interstitial velocities can be utilized due to their greater mechanical strength, this ratio grows even larger implying more substantial contributions of convection.

Convection-based drug delivery systems, such as localized injections and infusions, hold distinct transport advantages over delivery systems that rely heavily on diffusion for drug transport, like drug patches. First, barriers to diffusion can be circumvented by inserting appropriate catheters or needles into pre-determined depths. Thus, the requirements for i) excessively high drug concentrations to establish steep concentration gradients, and ii) prolonged time for macromolecules to diffuse across the barriers are eliminated. While concerns over the invasiveness of these processes may be raised, needles of appropriate sizes according to tissue type can be used to minimize the associated damage [26,27,59]. For example, needles with diameters of approximately 2 mm are commonly used for brain biopsies [60], 25 gauge Carr-Locke needles are used for injections in the GI tract during endoscopies [61] and 27 or 30 gauge needles are used for intravitreal injections [62]. In addition, the bypassed impermeable barriers prevent leakage of drugs back out of the tissues by diffusion, thereby reducing systemic toxic side effects [63,64].

Second, especially for larger molecules, convective mass transfer occurs significantly faster than diffusion, with molecules penetrating further from their delivery site [65,66]. Even with infusion rates of 4 μl/min in the brain, penetration depths of 1.5–2 cm were obtained after 2 h of infusion, while approximately 42 days would be required with pure diffusion, neglecting losses [26]. In addition, the convective flux is not a function of individual molecular properties; as a result, the concentration profiles are relatively independent of the molecular weights of solutes [26,31]. Particles ranging from small molecules such as contrast dyes to large molecules such as viruses [67,68] and liposomes with molecular weights on the range of MDas [69–71] are simultaneously transported by bulk fluid flow. During and after infusion, diffusion can distribute the delivered macromolecules even further. However, especially when metabolism and clearance are considered, the additional volume of distribution is approximately one order of magnitude smaller than that achieved by convection during infusion [26,31].

Third, convection-based methods provide uniform, homogeneous concentration profiles of drugs over a large volume [63]. This enables treatment of a larger volume of diseased tissue with lower maximum concentrations and lower total amounts of drug. This is in stark comparison to diffusion-based methods, where most of the drugs are concentrated near the sites of administration. In the case of planar diffusion from a drug patch, the resulting concentration profile can be expressed as:

$$\frac{C(x,t)}{C_0} \times \frac{1}{\phi} = erfc\left(\frac{x}{\sqrt{4Dt}}\right) exp(-Kt)$$

Where $C(x,t)$ is the concentration of drug at depth x and time t, C_0 is the initial concentration of drug in the drug source, ϕ is the volume fraction of interstitial fluid, *erfc* is the complementary error function, D is the diffusion coefficient of drug in the interstitial fluid, and $exp(-Kt)$ is the loss term, due to uptake and degradation. From this model, it is apparent that drugs are not effectively distributed to wide areas, but remain close to their reservoirs [72].

Fourth, utilizing convection imparts greater control over the spatiotemporal concentration profile [59,73,74]. From estimated profiles of how the infusate flows, the number of injection sites and flowrates can be controlled to deliver drugs only to the target sites, minimizing harmful off-target effects. For example, a commercially available, FDA-approved program called iPlan Flow can be used to estimate needle insertion sites for optimal drug distribution profiles in the brain [75]. iPlan Flow calculates the concentration profile at each time and point by solving a series of partial differential equations, which consider contributions of diffusion, convection and losses through metabolism and leakage. Main parameters such as the hydraulic conductivity and interstitial volume are obtained from magnetic resonance imaging (MRI) data of each patient. Then, using the boundary

conditions for pressure obtained from a mathematical model, the spatiotemporal concentration profile at each point, during and after the infusion is obtained [76]. Algorithms for determining the number and positions of infusion sites for reducing off-target effects can be developed for other systems too, not limited to CED [77]. In addition, while diffusion-based methods are pre-programmed, convection-based methods with controllable actuators such as infusion pumps allow for instant modifications regarding infusion and halting timepoints or flow parameters.

While convection-based methods have shown potential to overcome the limitations of diffusion-based methods, they too have limitations. Especially compared to diffusion-based methods such as nanoparticles which are typically intravenously administered, the placement and actuation of the device can be more invasive; surgery may be required

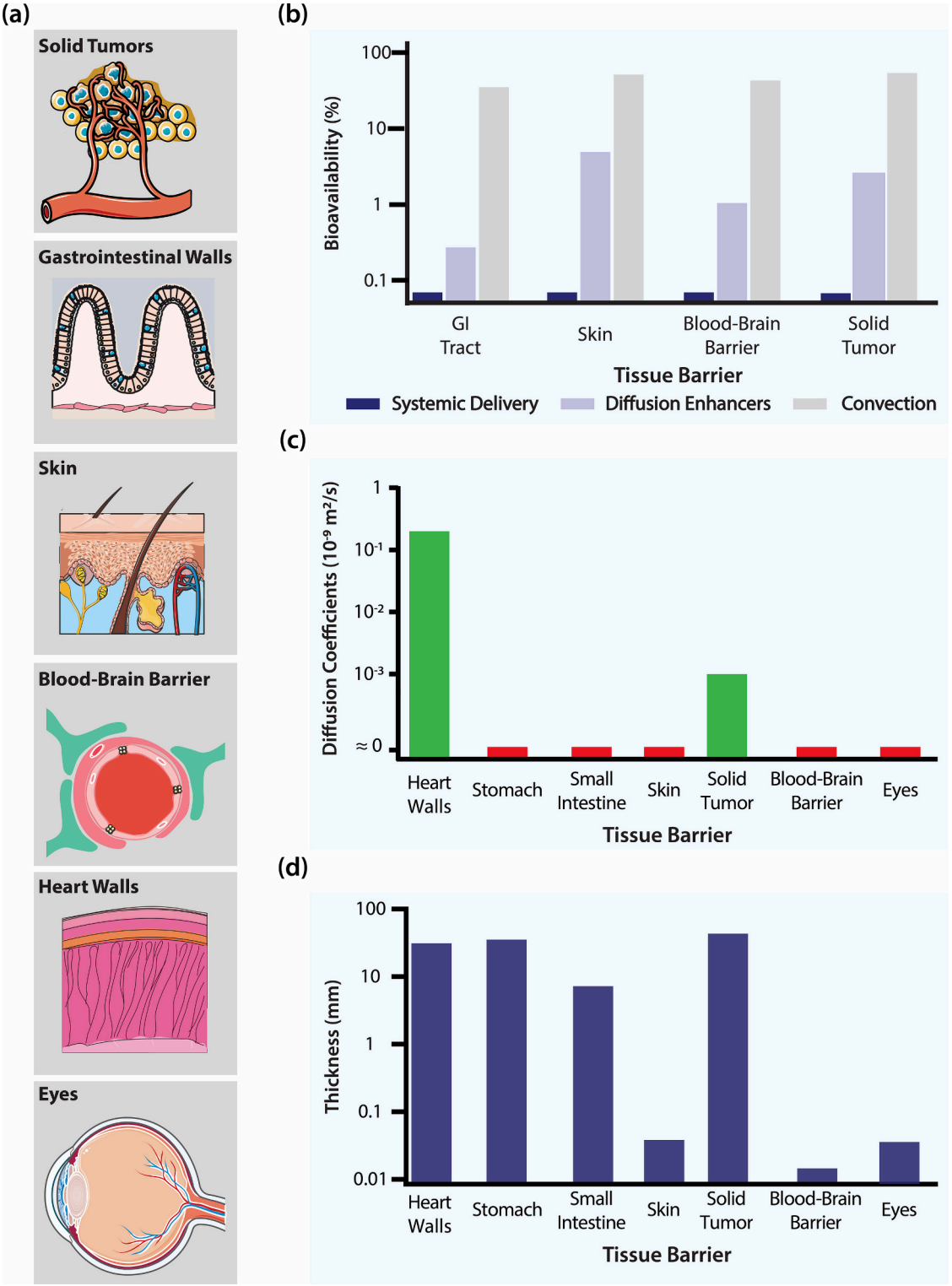

Fig. 2. Barriers to macromolecular penetration in the human body and their characteristics. (a) Illustration of diffusion barriers in the body. (b) Bioavailability of macromolecules across such barriers following various administration methods, (c) typical diffusion coefficients of penetrating macromolecules, and (d) the thickness of each barrier is compared. Parts of the figure were adapted from Servier Medical Art, CC BY license.

for the placement of the device, reducing patient acceptance rates while simultaneously increasing costs and the potential for surgical complications [26,59,78]. In addition, the mechanical disruption of the barrier by actuation of the device can compromise the integrity of barriers designed to prohibit entrance of pathogens or strictly regulate the transport of molecules [79–81], at times leading to microhemorrhages [27], nerve damage [82], infections or function loss. Furthermore, to avoid side effects due to excessive exposure or high concentrations of drug, including cytokine release syndromes and tissue damage at non-target sites [83], their distribution must be carefully controlled such that the drugs remain only within the target tissue.

Compared to diffusion-based methods, robotic devices enabling convective drug delivery can be more complex, difficult to design, and expensive as additional components for actuation must be incorporated. For example, convection-enabling devices require an actuation component that applies the required additional infusion pressure, such as a pump [26,59], a spring [27,84], an external plunger [78,85], or a gas generating chemical reaction [86–88]. Additional components such as triggering mechanisms, drug reservoirs, needles, biocompatible coatings, electronic microcontrollers, batteries, and others may also be required. Only recent advances in microfabrication and 3D printing have enabled the development of miniaturized devices capable of minimally invasive injections [27,59]. Design of the injection components must consider the additional pressure to overcome the mechanical resistance of the tissue, while minimizing backflow at the same time. This requires extensive mechanical tissue characterization studies during the design process. For triggerable or closed-loop systems, components for communicating with external stimuli or biosensors are also required [89]. As a result, the size and complexity of the device, in addition to costs that patients must bear, can be greater.

3. Barriers in the body

Numerous physiological barriers in the body constrain the modes by which drugs are administered and limit the efficacy of therapies (Fig. 2). For example, according to both healthcare professionals and patients, oral delivery is not only the most preferred, but also the most convenient mode of administration [24]. However, the walls and mucus layers of the GI tract, in addition to factors such as the low pH of the stomach and the abundance of digestive enzymes limit bioavailabilities of ingested peptide drugs to approximately 0.01–1% [6]. Furthermore, fear of needles and injections can lead to a delay in treatment initiation and lower patient adherence, compared to oral administration [90]. Thus, despite the clear advantages of oral administration, macromolecule administrations are typically limited to parenteral routes. In this section, we examine various diffusion barriers and how these barriers limit the efficacy of diffusion-based methods.

3.1. Skin

While the stratum corneum, the outermost layer of the epidermis, measures only 10–30 μm thick, it imposes significant barriers to transdermal drug delivery [91]. Its tight junctions and lipid bilayers prevent the transport of both hydrophilic molecules and molecules with molecular weights >500 Da [81,92]. For example, water's diffusion coefficient in the skin is $2.16 \pm 1.14 \times 10^{-13}$ m^2/s [93]. Even hydrophobic steroid hormones with molecular weights lower than 500 Da have diffusion coefficients of the same order of magnitude as that of water [94]. Larger macromolecules require an estimated 56 h to diffuse over the stratum corneum. Thus, when relying solely on diffusion, negligible transdermal macromolecule uptake occurs, as shown in multiple reports of macromolecule topical absorption [11,95]. Ionic liquids developed by Mitragotri and colleagues increase diffusive flux of drugs by replacing lipids in the stratum corneum with itself and water, but even after 24 h, <10% of the administered macromolecules reach the dermis and layers underneath [18].

3.2. GI tract

The mucosa layers, approximately 1.5 mm thick in the stomach [96] and 20–100 μm thick in the small intestine [97] act as barriers to macromolecular uptake by diffusion, while the submucosa and muscle layers underneath are highly vascularized and enable rapid systemic uptake via diffusion. The layers themselves are thin, and idealized equations suggest that complete penetration only requires timescales on the order of hours for macromolecules with diffusion coefficients on the order of 10^{-12} m^2/s. However, the tight junctions of the epithelial layers strictly regulate transport, and thus macromolecules larger than 5–10 Å do not absorb via paracellular diffusion [33,34]. Combined with the low pH of the stomach and the presence of digestive enzymes in the small intestine that rapidly degrade macromolecules, the GI tract largely prevents macromolecule uptake via diffusion. Scientists have developed complex formulations incorporating protease inhibitors [21] or chemical permeation enhancers such as ionic liquids [19,98], salcaprozate sodium (SNAC) [22,23] and sodium caprate (C10) [22] to enhance drug penetration across the gastrointestinal walls, but further strategies to increase bioavailability (typically <1% [6]) are required [23]. Srinivasan and colleagues developed an ingestible robotic device for enhanced drug delivery efficiency of peptides in the small intestine by effectively clearing the mucus lining, but the remaining epithelial diffusion barrier still limits systemic uptake to <1% of the loaded dose [99].

3.3. Brain

The BBB protects the brain and the central nervous system (CNS) from macromolecular diffusion. While the endothelial layer is only around 200 nm thick [100] and the basement membrane is 50–100 nm thick [79], transcellular transport of macromolecules is rare, and the endothelial layer's high density of tight junctions prevents fenestration [79]. As a result, neither the paracellular nor the transcellular pathway allows molecular transport; the BBB prevents passage of 98% of small molecules and nearly all macromolecules [100]. When intravenously administering most antibodies, just 0.01–0.1% of the serum concentration enters the brain [101]. Strategies to enhance transport across the BBB include exploiting receptor-mediated transcytosis pathways, such as targeting the transferrin receptor and insulin receptors. However, the high endogenous concentration of transferrin fully saturates the transferrin-binding sites prior to transferrin-drug conjugates, and as these receptors are not unique to the BBB, side effects such as hypoglycemia may arise [100]. In addition, studies show that the brain rapidly removes transferrin into the blood [102]; hence, strategies to prevent efflux from the brain must be developed. If significant amounts of drug do enter the brain, diffusing through the interstitial space to reach their target sites in the inner regions of the brain poses another challenge. Biomaterials such as hydrogels can be directly implanted in the brain via surgery, but rapid efflux by transporters can render the treatment ineffective. For example, when scientists injected antibodies intranasally, their concentration in the brain relative to 20 min post injection fell 50% after 40 min, and 95% after 90 min [103]. Alternate strategies such as utilizing cerebrospinal fluid (CSF) to enter the brain have been attempted [51,52,104]. Compared to the BBB, the leakier choroid plexus, the location where drug can enter the CSF, provides a superior drug entrance [105]. In addition, drugs can be injected at higher concentrations through intracerebroventricular injections. However, upon entering the brain, many drugs are rapidly transported out into the bloodstream [51]. In one study, half of intracerebrally injected antibodies were cleared from the brain after 48 min [53]. In addition, the rapid (4–5 times/day) turnover rate of the CSF limits the time available for drugs to diffuse into the inner regions of the brain [106]. As a result, not all small molecule drugs [107] and even fewer proteins [52,53,108] penetrate >1 mm into the parenchyma. Therefore, only a subset of small molecules whose transport is less hindered by diffusion, such as chemotherapies, utilize diffusion-based delivery

without significant issues.

3.4. Solid tumors

Especially with unresectable tumors, therapeutic agents must reach the inner core of tumors in addition to the periphery. However, uneven vascularization, slow interstitial diffusion, and elevated interstitial pressure make this challenging [28,29,109]. The well-vascularized tumor periphery possesses leaky blood vessels, facilitating extravasation of systemically administered drugs. In these regions, blood vessels appear every 200 μm, requiring drugs to only diffuse 100 μm to reach their target. However, compared to other tissues, the tortuosity of paths and interaction with components of the extracellular matrix slows diffusion in tumors [29,38]. As a result, in some tumors, liposomes and large dextrans with similar molecular weights diffuse too slowly for their diffusion coefficients to be measured by fluorescence recovery after photobleaching [38]. In another study, the diffusion coefficients of IgG molecules in carcinomas measured just 10^{-13}-10^{-12} m^2/s, resulting in a required interstitial diffusion timescale of 2 days for 1 mm. In addition, poorly vascularized regions, such as the (semi-) necrotic or hypoxic regions near the core of the tumor possess greater diffusion length scales. These solid mass regions formed by aggressive tumors grow faster than the rate at which new blood vessels are formed [110,111]. It is common for tumors to reach centimeter-scale sizes when diagnosed [112,113] and contain hypoxic regions ranging from 10 to 40% of the tumor [114,115]. Penetrating sparsely vascularized regions is challenging and time-consuming for macromolecules relying solely on interstitial diffusion; they require timescales of 7–8 months to penetrate 1 cm into solid tumor tissue [116]. In addition, diffusion into the core is countered by elevated interstitial fluid pressures at the core [28,29,45]; the high pressure causes interstitial fluid in tumors to flow towards the periphery, negating the inwards diffusion of drugs. This reduces the efficacy of anticancer treatments and may lead to treatment failure [117,118]. Furthermore, tumor cells regenerate rapidly [119], and tumor heterogeneity produces uneven drug distributions, both of which further diminish the efficacy of therapies. Together, these studies imply that patients require alternate drug delivery systems for rapid and efficient drug distribution over the entire tumor. Utilizing convection to penetrate solid tumors overcomes the aforementioned barriers; several studies indicate enhanced distribution profiles and treatments efficacies when healthcare professionals directly inject macromolecules into the tumor [120,121]. However, direct injection can lead to heterogeneous drug distributions, drug leakage, severe off-target side effects in the surrounding tissues, and disruption of the tumor microenvironment which may lead to higher rates of metastasis [122–125].

3.5. Heart walls

The 1.2–1.5 cm thick left ventricular free wall acts as a barrier which prevents diffusion-based methods from effectively treating myocardial infarctions [126]. In mice, the diffusion coefficients of a 40 kDa dextran molecule across the left ventricular free wall measure approximately 3×10^{-10} m^2/s and 1.8×10^{-10} m^2/s, before and after the onset of the fibrotic foreign body response, respectively [127]. If similar diffusion coefficients are observed in human tissue, it will require 7 and 12 days, respectively, for the model drug to diffuse across the left ventricular free wall from the epicardial surface of the left ventricle. Even if an injected hydrogel/drug formulation forms a bolus in the center of the myocardium, drug molecules will require 35 h to diffuse throughout the entire tissue wall depth. For larger drugs such as viral vectors [128] and liposomes [129], even longer periods will be required. In addition, previous studies show that the myocardium retains <50% of delivered drugs over time [130,131]. Thus, effective treatments require a rapid drug delivery system capable of distributing drugs to a large volume of the myocardium before clearance. Extended release hydrogel formulations and cardiac patches have been developed to deliver macromolecule drugs and cells to the heart to expedite wound healing following a myocardial infarction [132–135]. While many of these formulations demonstrate reduced scar tissue formation and increases in ejection fraction following delivery in small animals, they fail to achieve the same results in large animals [132,133,136]. This may be because large animals have left ventricular walls over ten times thicker than mice, providing a more formidable diffusion barrier [137]. Convection-based methods enable expedited distribution of drugs over large volumes of the myocardium with homogeneous spreading [138].

3.6. Eyes

The cornea, the 0.5 mm thick outermost layer of the anterior section of the eye [139], acts as the main barrier to ocular drug delivery [140]. Similar to the small intestinal epithelium and the BBB, the tight junctions present in the cornea prevent the passage of molecules [141,142]. For example, the bioavailabilities of even small molecule drugs typically measure <10% [142]. In addition, factors such as vision impairment and the rapid clearance of topically applied liquid formulations by blinking and tears further undermine diffusion-based ocular drug delivery [142,143]. Hanes et al. developed a gelling hypotonic polymer solution containing small molecule drugs which forms a thin, clear layer upon topical administration [143]. This formulation overcomes some of the aforementioned complications, but a system for macromolecules is yet to be developed. As a result, healthcare professionals utilize convection-based intravitreal injections for macromolecule administration, which deliver larger doses (approximately 100 μl) rapidly without impairing vision [144–146].

3.7. Fibrotic bodies

The fibrotic foreign body response generates another diffusion barrier that prevents macromolecules uptake from implanted devices such as hydrogels. Upon recognition of foreign bodies, recruited immune cells such as macrophages deposit proteins to form crosslinked fibrous layers encapsulating the biomaterial [147]. The deposited fibers and associated immune cells cause stress on the biomaterial, ultimately leading to material failure [148]. In addition, while the extent depends on the thickness of the fibrous capsule, the fibrous capsule can significantly decrease the flux of even small molecules including oxygen and glucose, such that their diffusion times are approximately doubled [149,150]. A similar retarding effect has been observed for macromolecules. For example, the diffusion coefficient of a 40 kDa dextran diffusing from a hydrogel attached to the epicardial surface of a mouse heart into the myocardium decreased by approximately 20% following only 20 days of being implanted [127]. Similar results were observed from subcutaneous devices containing insulin in mice [46]. Thus, this additional barrier to diffusion must be considered when delivering drugs for a sustained period, as onset of fibrosis occurs approximately 7 days following implantation [151]. The fibrotic foreign body response can be mitigated by altering the implant geometry or constituent polymers [47,152–154], and such systems are in the process of being commercialized. Robotic devices capable of oscillatory movements can be utilized to prevent fibrosis, while simultaneously increasing efflux of drugs from the device and its lifespan [46,155]. Convection-based methods can also be used to overcome the foreign body response by altering flow parameters to accommodate for the increased resistance to mass transport.

4. Clinical successes and failures of diffusion-based drug delivery systems

In this section, we discuss the successes and failures of hydrogel implants and nanoparticles in the context of the aforementioned physiological barriers (Fig. 3).

4.1. Hydrogel implants

The FDA has approved very few hydrogel implants that require their cargo to pass through a poorly permeable tissue barrier. At the time of our review, Vantas® (Endo Pharmaceuticals; discontinued in 2021) was the only injectable hydrogel for drug delivery to cancers to be approved by the FDA [5]. It was implanted in the subcutaneous space of the upper arm where a small molecule drug, histrelin acetate (1.3 kDa), would be released to suppress the growth of advanced prostate cancers by targeting the gonadotropin-releasing hormone receptors in the pituitary gland of the brain [156]. The drug would be released for a year, after which the implant would be replaced. Histrelin acetate is uniquely capable of crossing the BBB and reaching its target, and thus its reservoir can be implanted on the vascular side of the BBB. Due to its small size and low molecular weight its diffusive flux, even when hindered by the fibrotic foreign body response, is high enough to elicit a therapeutic response. The fact that only low concentrations (1.1 ng/ml) are enough to induce a response [157] also contributes to the implant's ability to suppress tumor growth.

As is evident from the fact that the only anti-cancer hydrogel approved by the US FDA for drug delivery delivers a relatively small peptide, histrelin acetate [5], hydrogels releasing larger proteins such as growth factors or monoclonal antibodies across physiological barriers have been less successful. This may be because the release rates of drugs from hydrogels are too slow and cannot establish sufficiently steep concentration gradients for macromolecules to penetrate the barriers. In addition, most hydrogels suffer from the fibrotic foreign body response, further limiting macromolecular diffusion out of the hydrogel [148,149]. For example, in treating advanced melanoma, 200 mg of pembrolizumab (tradename Keytruda®, Merck) in 8 mL of solution is typically dosed intravenously every 3 weeks. As hydrogels are mainly composed of water (70–99% [1]), delivering similar doses by hydrogels would require large gels of impractical size. In comparison, Vantas® contains 50 mg of histrelin acetate, which is released over a year.

4.2. Nanoparticles

Similarly to hydrogels, nanoparticle formulations that require passage across a poorly permeable tissue barrier have had limited to no success in the clinic, and FDA approved nanoparticle formulations target areas of the body that are easily reached from the administration site. In 2018, the US FDA approved patisiran (tradename Onpattro®), a nanoparticle drug encapsulating small interfering RNA (siRNA) for the treatment of polyneuropathy caused by amyloidosis of transthyretin (TTR) [158]. The lipid nanoparticles are modified such that following administration via intravenous infusion, apolipoprotein E (ApoE) is recruited in the bloodstream to increase specificity to and uptake by hepatocytes [159,160]. Once the nanoparticles enter the liver, they interact with ApoE-binding receptors on the surfaces of hepatocytes and are internalized, and siRNA is released. The detailed mechanism of action of the drug is not the scope of this review and can be found elsewhere [159,160]. The success of patisiran can be partly attributed to its target. In addition to the liver being a well-perfused organ, the liver's sinusoidal endothelial tissue is fenestrated [161]. This significantly

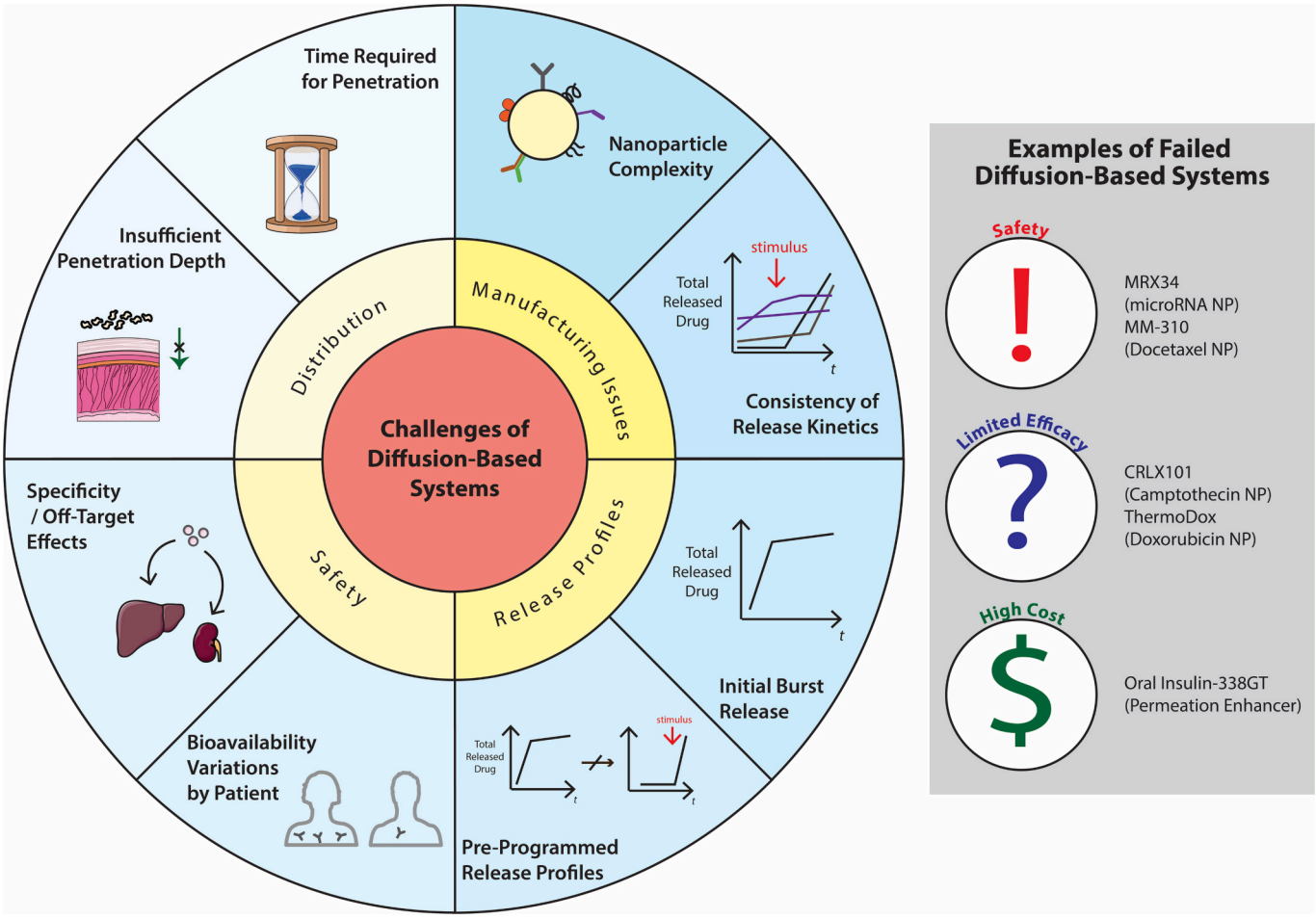

Fig. 3. Challenges associated with diffusion-based systems. Limitations of diffusion-based systems in the context of drug distribution, manufacturing issues, drug release profiles, and safety are illustrated along with examples of systems that have failed due to safety concerns, limited efficacy, and high cost of manufacturing. Parts of the figure were adapted from Servier Medical Art, CC BY license.

enhances paracellular permeability of large molecules and nanoparticles. A single dose of patisiran was shown to reduce serum TTR concentration by approximately 40% on average [159].

Covid-19 nanoparticle vaccines mRNA-1273 (Moderna) and BNT162b2 (BioNTech and Pfizer) have also successfully entered the clinic [162,163]. Here, lipids encapsulate mRNA encoding viral protein fragments. Unlike systemically distributed IV-administered nanoparticles, the lipid nanoparticle mRNA vaccines need not diffuse over long distances when distributed by convection throughout the muscle following an intramuscular injection. The vaccines can be taken up by both resident and recruited antigen-presenting cells (APCs) at the site of injection, which in turn enter the lymph nodes to initiate the cascade of immune responses [164]. In other words, as diffusion over physiological barriers is not required, the action of nanoparticles is not

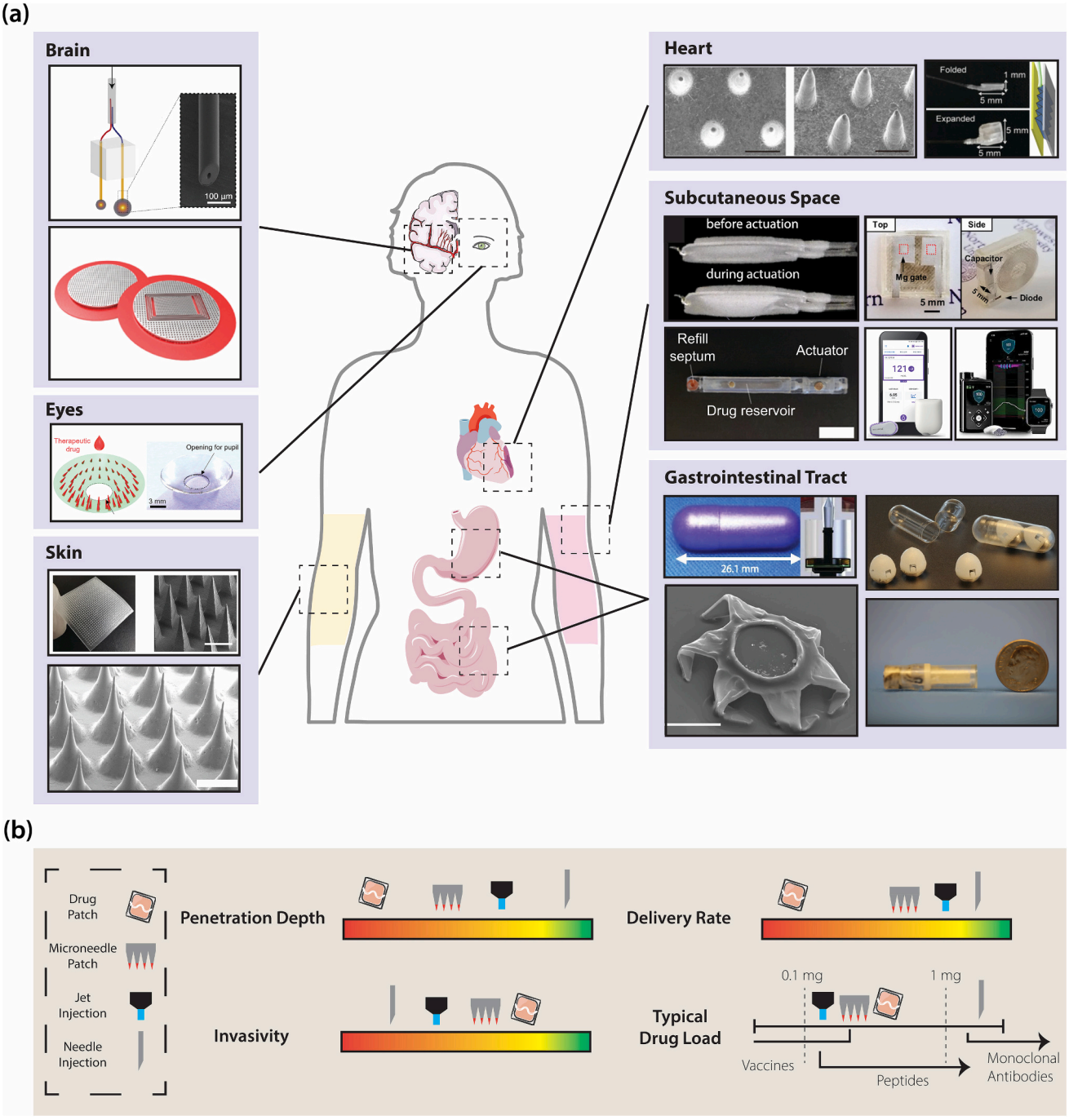

Fig. 4. Robotic drug delivery devices that break physiological diffusion barriers. (a) Various robotic drug delivery systems developed to overcome the limitations of diffusion-based systems and their actuation sites; (clockwise from top right) a microneedle patch for the heart [184], an origami heart pouch [192], the soft transport augmenting reservoir (STAR) [46], the wirelessly controlled battery-free implantable system (WCBIS) [193], MiniMed™ 780G (Medtronic), Omnipod® 5 (Insulet Corporation), a bioresorbable, wirelessly controlled subcutaneous implant [194], RaniPill™ [88], The liquid-injecting self-orienting millimeter-scale applicator (L-SOMA) [10,27,84], the theragripper [195], the luminal unfolding microneedle injector (LUMI) [168], a long-acting microneedle patch for reversible contraception [196], a glucose-responsive microneedle patch [197], a biodegradable lens with microneedles [198], a flexible, sticky, and wirelessly controlled drug patch for the brain [199] and a miniaturized neural drug delivery system (MiNDS) [59,74,77]. (b) Comparison of penetration depths, delivery rates, invasiveness, and typical drug loads of various robotic drug delivery devices and their potential applications. Parts of the figure were adapted from Servier Medical Art, CC BY license.

limited by their small diffusion coefficients. In addition, only small amounts of drug are typically required for vaccines; the Moderna vaccine and BioNTech and Pfizer vaccine contain only 100 μg and 30 μg of mRNA, respectively. Each vaccine was able to induce immune responses successfully; clinical trials measured vaccine efficacies of 95.2% and 95% for Moderna and BioNTech and Pfizer vaccines, respectively.

When diffusion barriers exist, nanoparticle drugs work less effectively. Doxil®, the first nanoparticle approved by the US FDA in 1995, treats ovarian cancer, AIDS-related Kaposi sarcoma and multiple myeloma. Compared to free doxorubicin, it shows either superior efficacy, reduced off-target toxicity or both due to the enhanced permeability and retention (EPR) effect [165]; the bulkiness of Doxil liposomes results in their accumulation primarily near tumors, whereas the small size and low molecular weight of free doxorubicin (543.52 g/mol) enables unhindered diffusion into most parts of the body and displays toxicity towards normal tissues. More efficacious compared to free doxorubicin, the response rate for recurrent ovarian cancer was limited to approximately 20% [166]. While the EPR effect may facilitate accumulation of the nanoparticles close to tumors, elevated interstitial pressures at the cores of tumors prevent transport of macromolecules accumulated at the periphery of tumors into the core, as previously discussed. Even when the elevated interstitial pressure is not considered, it is estimated that timescales of several months are required for immunoglobulins to diffuse 1–2 cm into the core; longer timescales are required for nanoparticles, due to greater hydrodynamic radii.

5. Fabrication methods for convective and diffusion-enhancing robotic systems

Fabrication methods such as 3D printing and microfabrication have expedited the development of customized, miniaturized, and sophisticated robotic devices. As a result of recent advances in these fields, many components and devices that either i) enable convective drug delivery, or ii) enhance the efficacy of diffusion-based methods by physically disrupting a physiological barrier have been developed [27,59,84,99,167,168]. In this section, we introduce physical tissue interfacing robotic devices that have been used to overcome diffusion barriers and enhance drug delivery profiles, and we note that systems utilizing convection in many cases provide superior pharmacokinetics and bioavailability to those that solely enhance diffusion (Fig. 4). Some of these components, designs, and devices are currently in clinical trials, while others may be incorporated into future convection-based systems to enhance their function and clinical translatability.

5.1. Convection-based methods

In this subsection, we explore various convection-based methods developed for each diffusion barrier and their limitations. (See Table 1)

5.1.1. Skin

Needle-free jet injections enable convection-based transdermal drug delivery. Injected drug solutions travel 100–200 m/s out of a nozzle smaller than 100 μm in diameter [169]. Approximately 100–500 μl of the drug solution penetrates into the subcutaneous space, where the drug is distributed. As the skin hosts a large population of immune cells [170], jet injections provide an efficacious vaccination delivery platform. Delivery of other macromolecules such as insulin [85] and monoclonal antibodies [171] have also been demonstrated. Polymeric particles have also been injected into the skin, with the encapsulated small molecules being released over approximately 3 weeks [172]. However, compared to conventional injections with hypodermic needles, reports indicate that needle-free jet injections cause swelling and erythema, as well as similar levels of pain [169]. In addition, jet injections' limited dosing capacity pales in comparison to subcutaneous injections, where antibody doses reach over 1000 mg per administration [173].

Table 1
Canonical convection-based methods for drug delivery across multiple physiological barriers and their characteristics.

Actuation Location	Device /Method	Mechanism		Device Size (Implanted/ Ingested)	Molecules	Dose (Volume)	Average Injection Velocity	Reference
		Delivery	Trigger					
GI Tract	Mouth	MucoJet	Needle-free; aqueous jet	Hydration	d : 7 mm h : 15 mm	Ovalbumin	100 μl	50–200 mm/s	[86]
	Stomach	L-SOMA	32G metal needle	Hydration	d : 12 mm h : 15 mm	Epinephrine, GLP-1 analog, Insulin, Adalimumab, Polymeric Nanoparticles	80 μl	~24,000 mm/s	[27,84]
Brain		CED	Safe metal needles or catheters	Manual	N/A	Peptides – Nanoparticles, Viruses	100–1000 μl	~0.84 mm/s	[63]
		MiNDS	Customized 200 μm needle	Manual	N/A	Muscimol	1 nl – 1 μl	0.04–0.4 mm/s	[59]
Eyes		I2T2	30G metal needle	Mechanical resistance change	N/A	CT Contrast Agent	~100 μl	~150–1850 mm/s	[146]

5.1.2. GI tract

Multiple convection-enabling robotic devices enable macromolecule delivery in the GI tract. In the mouth, a device called MucoJet developed by Aran and colleagues provides a needle-free jet injection into the cheek [86]. A hydration mechanism triggers a carbon dioxide generating chemical reaction, which ejects a vaccine solution that can penetrate the mucosal layer and elicit immune responses in rabbits.

In the small intestine, the RaniPill™ utilizes intestinal fluid to dissolve a membrane separating reactants [87,88]. This initiates a chemical reaction that produces carbon dioxide. The gas drives a dissolvable needle into the small intestinal walls, out of which the drug is injected. When delivering octreotide, the pill reached systemic bioavailabilities of ~65% [88], while bioavailabilities closely matching that of subcutaneous injections were observed when injecting insulin [87]. Delivering drugs across the stomach walls, compared to the small intestine, may enable faster and safer drug delivery; this is because actuation can take place prior to gastric emptying, which requires up to 4 h in a healthy stomach [174]. In addition, as the walls are much thicker in the stomach than in the intestine, less risk of perforation exists. The L-SOMA, an ingestible capsule developed by some of the authors of this paper, delivers drugs convectively by inserting a retractable needle and injecting liquid formulations of drugs including epinephrine, insulin, GLP-1 analogs, monoclonal antibodies, and mRNA-containing polymeric nanoparticles into the stomach submucosa [27,84]. Doses of up to 4 mg and absolute bioavailabilities of up to 80% were achieved in swine.

5.1.3. Heart

Engineers have developed needle-free injection systems to deliver drugs into the myocardium to treat myocardial infarctions and subsequent heart failure [78,175]. Compared to conventional injection methods, the jet injection method showed similar retention of drug in the left ventricle while minimizing systemic uptake of drug, quantified by liver exposure [175]. Delivery of adeno-associated viruses (AAVs) showed improved left ventricular ejection factors and thickening of the left ventricular free wall – signs of left ventricular reconstruction post-infarction [78]. Given that the macromolecules capable of stimulating regeneration of the heart post-infarction such as growth factors [127] and AAVs [78,175] have molecular weights on the order of 10 kDa to MDas, we expect convection-based methods to outperform diffusion-based methods for distribution of the drug throughout the diseased tissue.

5.1.4. Brain

For delivering drugs into the brain, a variety of pump systems have been developed. For example, Ramadi, Dagdeviren, and colleagues have developed a miniaturized neural drug delivery system (MiNDS) for drug delivery into the brain [59,74,77], while continuously recording neuronal electroencephalogram (EEG) activity. By implanting MiNDS in the brain, they bypassed the BBB while minimizing backflow and off-target effects. MiNDS convectively delivered muscimol, a γ-aminobutyric acid (GABA) agonist to the implanted region in microliter quantities, confirmed by EEG diagrams and changes in behavior. No significant immune response or necrosis was observed after 8 weeks, indicating feasibility of long term drug delivery for treating chronic neurological diseases with low invasiveness. Steerable microcatheters [176] and probes [73] have also been developed for precise targeting. In this study, the angle at which the needle is inserted was demonstrated to affect the trajectory of drug solutions [73].

5.1.5. Eyes

While intravitreal injections are widely utilized for the administration of macromolecular drugs such as Eylea® and Lucentis®, complications such as lack of specificity and drug leakage can be overcome by utilizing electromechanical devices to target specific regions of the eye [142,144]. A method developed by Prausnitz et al. enables selective targeting of the posterior region of the suprachoroidal space by delivering negatively charged nanoparticles through hollow microneedles followed by iontophoresis for the translocation of nanoparticles [145]. In this way, >30% of the administered nanoparticles were delivered specifically to the posterior region in rabbits. Furthermore, electromechanical devices for targeting the eye can provide enhanced sensitivity compared to human operators when determining the optimal position and timing of the injection. For example, the intelligent injector for tissue targeting (I2T2), a resistance-sensing injector developed by Karp et al., determines the optimal needle insertion site based on changes in force required to advance the needle [146].

5.1.6. Fibrotic foreign bodies

When implanted devices deliver drugs for prolonged periods, the fibrotic foreign body greatly reduces the efficiency of diffusion-dependent drug delivery systems [47,147,153]. To attenuate the fibrotic foreign body response, Roche and colleagues developed a soft transport augmenting reservoir (STAR) [46] composed of a therapeutic chamber, an actuation chamber, and an outer layer. The pressure within the actuation chamber can be continuously controlled such that it inflates and deflates rapidly to oscillate. This intermittent actuation significantly reduces the formation of fibrotic layers, extending the lifespan of the implant without losing functionality. In addition, by disturbing the surrounding fluids via oscillations, added convective mass transfer contributions accelerate drug elution from the implant compared to simple diffusion. As a result, insulin was consistently delivered for over 8 weeks.

5.2. Diffusion-enhancing methods

While the following devices ultimately depend on diffusion for distribution of drug, these devices facilitate distribution by incorporating functions such as mechanically disrupting physiological barriers or continuously maintaining maximal concentration gradients. Although these devices have drawbacks such as limited drug loading and less control over the spatiotemporal concentration profile compared to convection-based methods, they distribute drugs further than passive diffusion-based methods. In addition, these devices incorporate many features that can be adopted by novel convection-enabling robotic drug delivery devices to further enhance their efficacy.

5.2.1. Skin

Solid microneedle formulations enhance diffusive flux by physically penetrating the stratum corneum and epidermis, essentially removing the initial barriers to transdermal diffusion. The dermis, due to its immense vasculature [126], is one of the few locations where delivery of diffusion-based methods which break through the stratum corneum provide similarly rapid uptake to convective delivery. Microneedles can be tuned to alter drug release kinetics and mechanisms. For example, drugs can be delivered in a single burst within a few hours [177], multiple bursts over days [178], or in a sustained manner for over six months [179]. In addition, microneedle patches can be incorporated within complex devices for closed-loop control of diseases. For example, Lee et al. report a wearable microneedle patch for closed-loop control of diabetes [167]. At elevated sweat glucose concentrations, a thermal actuator heats a microneedle patch and induces a phase change of the coating, thereby controlling the release rate of metformin, a drug used for controlling diabetes. Thus, blood glucose levels are controlled by a closed feedback loop. However, the limited volume of these devices for drug loading reduces the amount of total delivered drug by up to an order of magnitude. These microneedle formulations possess drug loads on the order of 100-μg [91,178,180], compared to gram-level doses through subcutaneous injections [173].

5.2.2. GI tract

For drug delivery in the GI tract, many diffusion-based robotic

devices disrupt the diffusion barriers with components such as microneedles. Latching onto and penetrating tissue walls shortens the diffusion length and enhances the residence time of drug within the GI tract, providing ample time for diffusion of small molecules and single kDa sized macromolecules. Although these devices are limited to moderate doses and cannot deliver larger macromolecules such as monoclonal antibodies and polymeric or lipid nanoparticles at therapeutically relevant concentrations, the design of these devices and their triggering mechanisms will inspire future ingestible robotic pills for convective drug delivery. Babaee et al. report multiple robotic devices for drug delivery in the esophagus, including a temperature-triggered flower-like device capable of delivering small molecules by inserting dissolvable drug-loaded millineedles into the esophagus [181] and a pressure-triggered kirigami-inspired stent that inserts barbs coated with polymeric nanoparticles [182]. Srinivasan and colleagues have developed a robotic device called RoboCap, an ingestible capsule that rotates against the small intestinal walls, clearing away mucus layers while topically depositing drugs [99]. As a result, 20- to 40-fold greater bioavailabilities are achieved for insulin in swine. Another microneedle-based robotic pill, the LUMI, was designed such that regardless of its orientation within the small intestine, its microneedles would penetrate the small intestinal walls upon release from its capsule, eliminating the need for external guidance [168]. The LUMI possesses three arms coated in microneedles which unfold in the small intestine after being triggered by a pH change. The device has been shown to deliver drugs such as insulin rapidly compared to subcutaneous injections, while achieving >10% bioavailabilities in swine.

While these barrier breaking devices increase bioavailability by one to two orders of magnitude more than chemical permeation enhancers, they are limited in their ability to deliver rapid acting pharmacokinetics, high peak plasma concentrations, and drug loads comparable to their liquid dosing counterparts. For example, the SOMA system described above was shown to deliver both solid and liquid insulin formulations [10,27]. While both possessed similar bioavailabilities compared to subcutaneous injections of the same formulations, the solid formulation delivered just 300 μg of drug (with a maximum loading capacity of 1–2 mg) [10] whereas the liquid formulation demonstrated up to 4 mg of drug loading [27]. Furthermore, the solid formulation delivered its payload over multiple days with a sustained release profile, while the liquid formulation reached a peak plasma concentration with 30 min following administration and demonstrated a rapid acting pharmacokinetic profile.

5.2.3. Heart

Many diffusion-enhancing systems with robot-like modifications for treating myocardial infarctions have been developed. Whyte and colleagues developed an implantable system called Therepi for sustained delivery of drugs from a hydrogel attached to the epicardial surface of the heart [127]. Unlike other hydrogels, the device is connected to a subcutaneous port by a refill line. The Therepi is continuously replenished with drug to maintain the maximal concentration gradient of drug across the hydrogel-tissue interface, the driving force for diffusive drug delivery. In addition, by injecting different drug formulations into the subcutaneous port, different drugs including small molecules, growth factors, and cells can be delivered at different timepoints, whereas other hydrogels are pre-programmed and lack this versatility. Huang et al. report another epicardial patch called PerMed [183], which consists of a biodegradable elastic patch with mechanical properties similar to the heart, and networks of microchannels for drug permeation. Sustained release of a growth factor from PerMed demonstrated enhanced revascularization and improvements in cardiac function. Drug-loaded epicardial microneedles have also been developed. Shi et al. report a microneedle-based device for gene therapy delivery using AAVs [184]. In rats, compared to bolus injections where the transfected cells were primarily located within a 500 μm distance, the swelling microneedles could deliver AAVs over a longer distance, approximately 3 mm, and displayed enhanced left ventricular function recovery. Microneedles for delivering cardiac stromal cells have also been developed [185]. In addition to delivering drugs, recent studies demonstrate the ability of hydrogels to provide mechanical support and ECM-mimicking environments to the infarct to accelerate revascularization and growth [186,187].

While these systems provide localized delivery to the heart at therapeutically relevant concentrations, they fail to provide the depth of penetration necessary to reach all areas of impacted tissue following a myocardial infarction. Microneedle systems improved drug penetration depth [184,185], but they only penetrated a distance equivalent to 20% of the thickness of a large animal's left ventricle. Furthermore, while port-based systems allowed for convective refilling of drugs, the reliance on diffusion for tissue penetration limited the penetration depth of the administered therapy to just 300 μm [127,183].

5.3. Examples of synergy between convection-based & diffusion-based systems

By utilizing the advantages of both convection-based and diffusion-based systems, greater therapeutic effects can be achieved. Convection-based systems can be utilized to overcome physiological barriers and diffusion-based systems can be exploited for sustained or targeted delivery. For example, the unique design of the L-SOMA, enabling oral delivery of macromolecules by circumventing the stomach lining, was combined with nanoparticles optimized for transfection. By changing the formulation of the nanoparticle, it may be possible to change the type of cell targeted by the nanoparticle [9]. Similarly, CED was used to deliver polymeric nanoparticles in the brain over a large volume [69–71], and intramuscular (local) injections of the Pfizer/BioNTech and Moderna lipid nanoparticle COVID-19 vaccines [162,163] removed the necessity of nanoparticles to extravasate from blood vessels and diffuse to their targets. Hydrogel injecting robotic devices have also been developed [188], where the hydrogel can be utilized for prolonged release of drugs, triggerable release by various stimuli, or mechanical support. Further progress in both systems will enable development of hybrid robotic devices with even greater control over the spatiotemporal drug concentration profile.

6. Tuning physical interactions

To treat the whole of diseased tissue by convective drug delivery while minimizing off-target effects, it is critical to understand how fluids are distributed upon injection and to control the pertinent variables. For example, suboptimal catheter positioning largely contributed to the underwhelming result of the PRECISE (Phase III Randomized Evaluation of CED of IL13PE38QQR with Survival Endpoint) clinical trial [189]; simulations by iPlan Flow showed that only 49.8% of catheters were positioned optimally. In addition to catheter positioning, other variables such as viscosity of the infusate and infusion rate can alter how fluids are distributed [64,190,191]. Here, we discuss some of the controllable variables in convective drug delivery (Fig. 5).

6.1. Viscosity

From Darcy's law $\left(q = -\frac{k}{\mu}\nabla p\right)$, it can be drawn that flowrates track inversely with viscosity at a given pressure gradient. As a result, low-viscosity formulations readily enter interstitial spaces and penetrate further into tissues in less time. In addition, smaller catheters, needles, and pumps can be used due to the fluid's lower resistance to flow, which are more suitable for miniaturization and implantation [190]. However, studies show that low-viscosity infusates commonly suffer from increased backflow, leakage, and lower distribution volumes [191]. Thus, high-viscosity formulations may be more suitable for treating larger diseased tissue volumes and low-viscosity formulations more

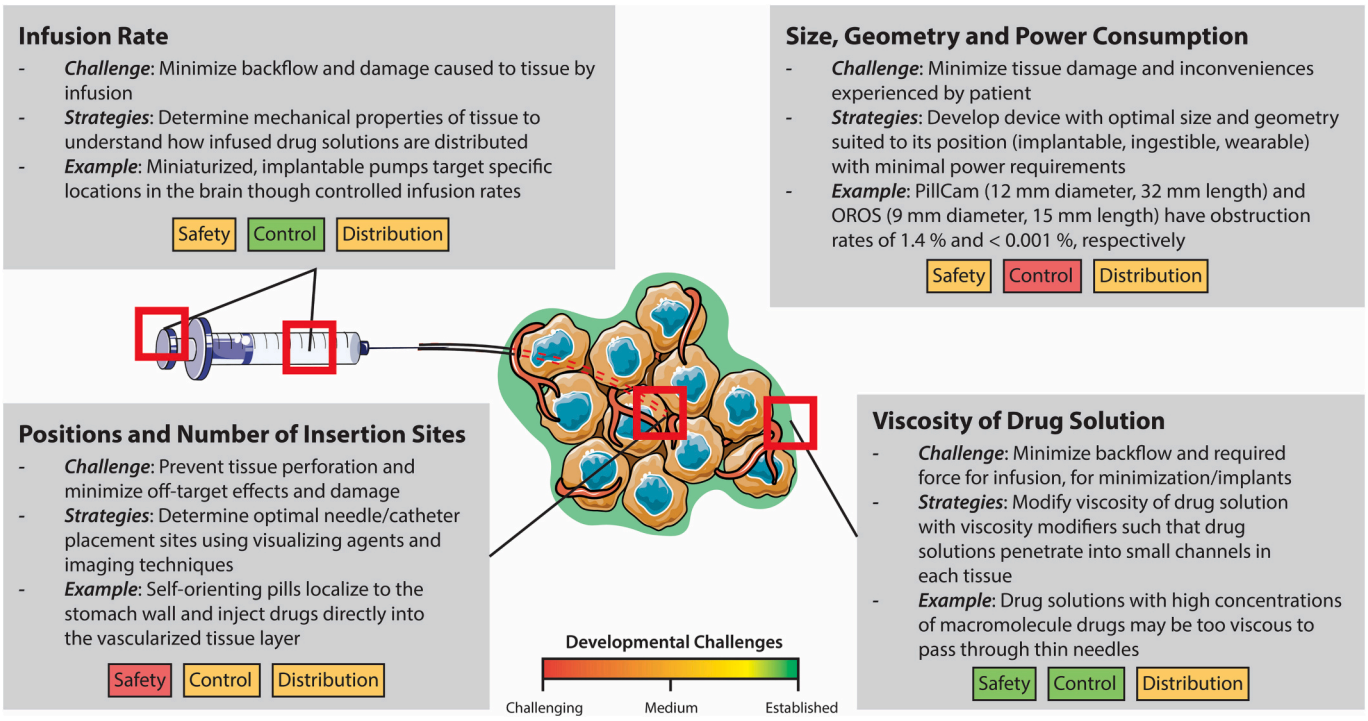

Fig. 5. Factors to be considered when developing convection-based systems. Associated developmental challenges and strategies to overcome the challenges are illustrated with a syringe and tumor. Parts of the figure were adapted from Servier Medical Art, CC BY license.

suitable for smaller tissue volumes with high densities of narrow interstitial sites. By adding viscosity modifiers such as polyethylene glycol or sugars, the viscosity of the formulation can be modified according to its purpose [190].

6.2. Infusion volume

Increasing the total infused volume increases the volume of distribution and the amount of drug delivered. In the brain, the volume of distribution initially increases linearly with the volume of infusion [26]. However, the volume of distribution eventually plateaus. Depending on physical properties of the tissue such as porosity, structure, and how tightly the layers are packed, each tissue's capacity to accept liquids within a set period differs. Once a total volume exceeding that capacity is delivered, backflow or leakage to adjacent tissues occurs; excess drugs will be wasted, and off-target toxicity will arise. For example, when the same volume of drug was injected into the stomach wall mucosa, only 40–50% of the dose remained, whereas 100% of the dose was retained when injected into the stomach submucosa [27]. Large infusion volumes can cause other complications, such as the dissemination of cells in relatively loosely packed tumors, causing metastasis [124,125]. Thus, determining the optimal total infused volume that maximizes distribution while minimizing tissue damage and backflow is critical.

6.3. Infusion rate and interstitial fluid velocity

At higher infusion rates, less time is required to deliver the same volume of infusate. However, similarly to high infusion volumes, high infusion rates cause significant backflow [64]. In addition, tissue damage and complications, such as tumor metastasis, can be observed at higher flow rates [124,125]. When determining the infusion rate, the physical properties of the tissues must be considered. For example, the L-SOMA safely injects 80 μl of drug into the gastric mucosa within milliseconds [27]. However, infusion rates are typically in the range of 0.1 to 10 μl/min for CED in the brain, due to the drastically softer nature of the tissue [64]. To minimize backflow, bolus formation, or tissue damage due to excessive swelling, the infusion rate must be equal to or less than the rate at which the infused fluid distributes within the tissue. This rate is calculated by summing the flowrates across all the channels formed. Thus, understanding the dimensions of and the distance between the channels formed in the tissue by the infused fluids is critical. At a given infusion rate, factors such as the dimensions of the infusion cannula or needle, porosity of the tissue, and interstitial pressure can affect the velocity of the infused fluid. Especially when delivering a drug that is toxic to normal tissue, these parameters must be chosen such that the fluid is distributed only throughout the target tissue without leaking. However, drastically reducing the infusion rate and interstitial fluid velocities can have adverse effects – excessive infusion times may be required, which can be burdensome for surgeries. Also, pathogens and undesired molecules may flow through the opened pathway during extended infusion sessions if the barriers are mechanically disrupted.

6.4. Depth, angle, and position

Needles or catheters inserted at different angles and depths deliver drugs to different tissue layers. As different tissues have varying distribution profiles (bolus, dispersed) and capacities to accept liquids, it is critical to predetermine the appropriate depth and angle of insertion. This can be done by injecting visualizing agents such as contrast dyes or radioisotopes and utilizing imaging techniques such as MicroCT [26,27] and MRI [75]. For example, the length of needles in the L-SOMA device was determined so that liquids were only injected into the submucosa or muscle layer of the stomach, instead of the mucosa [27]. While inserting needles or catheters deeper reduces the distance that drugs diffuse over, clear upper limits exist to prevent complete thickness perforations and excessive tissue damage. Other factors such as tissue heterogeneity and anisotropy must also be considered, as these alter the direction of fluid flow within the tissue [190]. Especially when delivering drugs into vital organs with limited regenerative capacity such as the brain and heart, scientists must understand how the infused fluids are distributed and generate methods to accurately determine the optimal position and orientation of the drug delivery device. However, as has been shown

from the retrospective analysis of the failure of the PRECISE trial [189], excessive device and positioning complexity can also lead to failure. Minimizing the complexity of the device assembly, placement, and operation may lead to reduced opportunities for clinician error, easier integration with current surgical procedures, reduced surgery times, and better health outcomes. When catheters or cannulae are inserted, the number of insertion sites can be determined and minimized prior to the surgery by imaging procedures and simulation software that utilize diffusion and convection drug delivery models specific to the targeted tissue. Additionally, insertion sites can be marked before the procedure to prevent misplacement. Components that must be inserted in a specific orientation or direction can be clearly marked and tracked during surgery, or devices can perform insertion passively and autonomously to minimize clinician error. For example, the SOMA capsule possesses a passively self-orienting geometry for localization, a passively triggered compressed spring for needle insertion, and a solid drug post for delivery [10]. Delivery depth is controlled by the length the spring can expand, drug delivery rate is determined via the post formulation, and tissue localization is performed autonomously by gravity. Future systems that utilize passive and self-actuating components may help to reduce device complexity, cost, and potential for dosing errors.

7. Outlook & conclusions

In this Review, we assess the limitations of diffusive mass transfer in the context of macromolecular drug delivery across poorly permeable tissue barriers and describe how convection-enabling robotic systems improve drug bioavailability and therapeutic efficacy compared to passive formulations. Convection-based methods have already shown success in bypassing the BBB [26,59] and the GI tract tissue walls [27,84]. Further demonstration of efficacy across solid tumors and the heart may provide new modes of drug transport that enable safe and effective therapies for diseases with poor prognoses. Moreover, characterizing how fluids are distributed in both healthy and diseased tissues through imaging procedures could enable personalized delivery profiles that reduce off-target side effects, maximize dose concentration in relevant tissues, and provide temporal control of dosing regimens.

Robotic device-based convective delivery naturally requires more invasive procedures compared to formulation based oral or systemic administration. While the safety of CED has been shown through extensive experimentation and clinical trials, the systems have been limited to extremely low flowrates in the brain, typically on the order of 1 μl/min [26,64,190]. When assessing new tissues for convective delivery, scientists must determine the appropriate needle sizes and flow parameters while also considering parameters such as interstitial pressure, thickness, potential for regeneration, and risk of infection. Long-term effects such as fibrotic encapsulation must also be considered when developing implantable systems for prolonged drug delivery to treat chronic diseases. Fibrous capsules can block the outlets of needles and catheters, and the additional pressure to force the liquid through these blockages needs characterization.

The final factors to consider are medical expertise requirements and cost. Some applications of convective drug delivery require surgical procedures. Excessive complexity of device placement can reduce the efficacy of therapies and even cause additional tissue damage, as has been learned from the retrospective analysis of CED trial data [189]. Furthermore, these involved procedures increase the cost of using such devices. Developing automated methods for device placement and implantation will significantly enhance the efficacy and reproducibility of treatment. In addition to placement complexity, electromechanical devices possess several moving parts which increase the manufacturing and assembly costs compared to diffusion-based methods. As advancements in additive manufacturing processes such as 3D printing continue to improve and the clinical adoption of devices becomes more prevalent, the increased volume and speed of manufacturing may lower these costs. However, device-based treatment may always remain more expensive than other materials-based solutions.

Recent innovations in biosensors and in vivo communication protocols hint towards the transition of traditional drug delivery systems to closed-loop systems in which drug delivery devices can be triggered by external sensors [89]. However, there exist several barriers to realizing fully automated systems, including: the development of communication protocols between sensors and drug delivery actuators; improvements in power management; and the development of micro-actuators that can be placed at sites of interest such as the heart, the brain, and solid tumors. Especially when diffusion barriers are present, convection-based methods have demonstrated superior bioavailabilities, distribution profiles, and spatiotemporal dosing control compared to diffusion-based systems [31,59,75]. Already, these advantages have been applied to oral macromolecule pills, brain drug delivery pumps, and other devices with immediate clinical applications. In the future, development of convection-enabling robotic devices may enable closed-loop control of many complex diseases and contribute to improving our quality of life.

CRediT authorship contribution statement

Jihoon Park: Writing – review & editing, Writing – original draft, Formal analysis, Conceptualization. **Ramy Ghanim:** Writing – review & editing, Writing – original draft. **Adwik Rahematpura:** Writing – review & editing, Writing – original draft. **Caroline Gerage:** riting – review & editing, Writing – original draft. **Alex Abramson:** Writing – review & editing, Supervision, Funding acquisition, Conceptualization.

Declaration of competing interest

A.A. is a co-inventor on ingestible devices for drug delivery. A.A. is a consultant for Novo Nordisk on ingestible drug-delivery devices. A full list of A.A.'s competing interests can be found here: https://www.abramsonlab.com/aa-conflicts-of-interest.

Data availability

No data was used for the research described in the article.

Acknowledgments

All images in the figures are collected from open-source scientific articles under CC BY licenses that enable the free reproduction of images in future scientific articles. Photo credits for the images are as follows: Graphical Abstract, from top to bottom, Khalil B. Ramadi, William Whyte, Alex Abramson, Arvinder K. Dhalla, and Fig. 4 (a), clockwise from top right, Hongpeng Shi, Xuan Mei, William Whyte, Jahyun Koo, Medtronic, Insulet Corporation, Seung Ho Lee, Arvinder K. Dhalla, Alex Abramson, Alex Abramson, Arijit Ghosh, Wei Li, Changwei Yang, Woohyun Park, Jongha Lee, and Khalil B. Ramadi. Parts of all figures were drawn by using pictures from Servier Medical Art. Servier Medical Art by Servier is licensed under a Creative Commons Attribution 3.0 Unported License (https://creativecommons.org/licenses/by/3.0/). A. A. thanks the financial support by the National Institutes of Health (R35GM150689), the Georgia Institute of Technology Institute for Electronics and Nanotechnology (1000x Seed Grant), and the Georgia Regenerative Engineering and Medicine Center.

References

[1] J.Y. Li, D.J. Mooney, Designing hydrogels for controlled drug delivery, Nat. Rev. Mater. 1 (2016).
[2] N.A. Peppas, J.Z. Hilt, A. Khademhosseini, R. Langer, Hydrogels in biology and medicine: from molecular principles to bionanotechnology, Adv. Mater. 18 (2006) 1345–1360.
[3] S.N. Bhatia, X. Chen, M.A. Dobrovolskaia, T. Lammers, Cancer nanomedicine, Nat. Rev. Cancer 22 (2022) 550–556.
[4] A.C. Anselmo, S. Mitragotri, Nanoparticles in the clinic: An update post COVID-19 vaccines, Bioengi. Translat. Med. 6 (2021).

[5] A. Mandal, J.R. Clegg, A.C. Anselmo, S. Mitragotri, Hydrogels in the clinic, Bioengi. Translat. Med. 5 (2020).
[6] A. Fjellestad-Paulsen, P. Höglund, S. Lundin, O. Paulsen, Pharmacokinetics of 1-deamino-8-d-arginine vasopressin after various routes of administration in healthy volunteers, Clin. Endocrinol. 38 (1993) 177–182.
[7] S. Wilhelm, A.J. Tavares, Q. Dai, S. Ohta, J. Audet, H.F. Dvorak, W.C.W. Chan, Analysis of nanoparticle delivery to tumours, Nat. Rev. Mater. 1 (2016).
[8] D.J. Brayden, The centenary of the discovery of insulin: an update on the quest for oral delivery, Front. Drug Deliv. 1 (2021) 726675.
[9] M. Hinchcliffe, L. Illum, Intranasal insulin delivery and therapy, Adv. Drug Deliv. Rev. 35 (1999) 199–234.
[10] A. Abramson, E. Caffarel-Salvador, M. Khang, D. Dellal, D. Silverstein, Y. Gao, M. R. Frederiksen, A. Vegge, F. Hubalek, J.J. Water, A.V. Friderichsen, J. Fels, R. K. Kirk, C. Cleveland, J. Collins, S. Tamang, A. Hayward, T. Landh, S.T. Buckley, N. Roxhed, U. Rahbek, R. Langer, G. Traverso, An ingestible self-orienting system for oral delivery of macromolecules, Science 363 (2019) 611-+.
[11] A.R. Tadros, A. Romanyuk, I.C. Miller, A. Santiago, R.K. Noel, L. O'Farrell, G. A. Kwong, M.R. Prausnitz, STAR particles for enhanced topical drug and vaccine delivery, Nat. Med. 26 (2020) 341–347.
[12] B. Belardi, T. Hamkins-Indik, A.R. Harris, J. Kim, K. Xu, D.A. Fletcher, A weak link with actin organizes tight junctions to control epithelial permeability, Dev. Cell 54 (2020) 792–804 (e797).
[13] H.J. Lemmer, J.H. Hamman, Paracellular drug absorption enhancement through tight junction modulation, Expert Opin. Drug Deliv. 10 (2013) 103–114.
[14] R.J. Boado, Y. Zhang, Y. Wang, W.M. Pardridge, Engineering and expression of a chimeric transferrin receptor monoclonal antibody for blood–brain barrier delivery in the mouse, Biotechnol. Bioeng. 102 (2009) 1251–1258.
[15] S.G. Patching, Glucose transporters at the blood-brain barrier: function, regulation and gateways for drug delivery, Mol. Neurobiol. 54 (2017) 1046–1077.
[16] K. Ulbrich, T. Knobloch, J. Kreuter, Targeting the insulin receptor: nanoparticles for drug delivery across the blood–brain barrier (BBB), J. Drug Target. 19 (2011) 125–132.
[17] I. Tamai, Oral drug delivery utilizing intestinal OATP transporters, Adv. Drug Deliv. Rev. 64 (2012) 508–514.
[18] Q.M. Qi, S. Mitragotri, Mechanistic study of transdermal delivery of macromolecules assisted by ionic liquids, J. Control. Release 311 (2019) 162–169.
[19] A. Banerjee, K. Ibsen, T. Brown, R. Chen, C. Agatemor, S. Mitragotri, Ionic liquids for oral insulin delivery, Proc. Natl. Acad. Sci. 115 (2018) 7296–7301.
[20] T.D. Brown, K.A. Whitehead, S. Mitragotri, Materials for oral delivery of proteins and peptides, Nat. Rev. Mater. 5 (2020) 127–148.
[21] R. Eldor, J. Neutel, K. Homer, M. Kidron, Efficacy and safety of 28-day treatment with oral insulin (ORMD-0801) in patients with type 2 diabetes: a randomized, placebo-controlled trial, Diabetes Obes. Metab. 23 (2021) 2529–2538.
[22] C. Twarog, F. McCartney, S.M. Harrison, B. Illel, E. Fattal, D.J. Brayden, Comparison of the effects of the intestinal permeation enhancers, SNAC and sodium caprate (C10): isolated rat intestinal mucosae and sacs, Eur. J. Pharm. Sci. 158 (2021) 105685.
[23] S. Maher, C. Geoghegan, D.J. Brayden, Intestinal permeation enhancers to improve oral bioavailability of macromolecules: reasons for low efficacy in humans, Expert Opin. Drug Deliv. 18 (2021) 273–300.
[24] A. Abramson, F. Halperin, J. Kim, G. Traverso, Quantifying the value of orally delivered biologic therapies: a cost-effectiveness analysis of oral semaglutide, J. Pharm. Sci. 108 (2019) 3138–3145.
[25] I.B. Halberg, K. Lyby, K. Wassermann, T. Heise, E. Zijlstra, L. Plum-Mörschel, Efficacy and safety of oral basal insulin versus subcutaneous insulin glargine in type 2 diabetes: a randomised, double-blind, phase 2 trial, Lancet Diabetes Endocrinol. 7 (2019) 179–188.
[26] R.H. Bobo, D.W. Laske, A. Akbasak, P.F. Morrison, R.L. Dedrick, E.H. Oldfield, Convection-enhanced delivery of macromolecules in the BRAIN, Proc. Natl. Acad. Sci. U. S. A. 91 (1994) 2076–2080.
[27] A. Abramson, M.R. Frederiksen, A. Vegge, B. Jensen, M. Poulsen, B. Mouridsen, M.O. Jespersen, R.K. Kirk, J. Windum, F. Hubalek, J.J. Water, J. Fels, S. B. Gunnarsson, A. Bohr, E.M. Straarup, M.W.H. Ley, X.Y. Lu, J. Wainer, J. Collins, S. Tamang, K. Ishida, A. Hayward, P. Herskind, S.T. Buckley, N. Roxhed, R. Langer, U. Rahbek, G. Traverso, Oral delivery of systemic monoclonal antibodies, peptides and small molecules using gastric auto-injectors, Nat. Biotechnol. 40 (2022), 103-+.
[28] R.K. Jain, Physiological barriers to delivery of monoclonal-antibodies and other macromolecules in tumors, Cancer Res. 50 (1990) S814–S819.
[29] R.K. Jain, Transport of molecules in the tumor INTERSTITIUM - a review, Cancer Res. 47 (1987) 3039–3051.
[30] A. Schudel, D.M. Francis, S.N. Thomas, Material design for lymph node drug delivery, Nat. Rev. Mater. 4 (2019) 415–428.
[31] P.F. Morrison, D.W. Laske, H. Bobo, E.H. Oldfield, R.L. Dedrick, High-flow microinfusion - tissue penetration and pharmacodynamics, Am. J. Phys. 266 (1994) R292–R305.
[32] D. Günzel, A.S.L. Yu, Claudins and the modulation of tight junction permeability, Physiol. Rev. 93 (2013) 525–569.
[33] L. Shen, C.R. Weber, D.R. Raleigh, D. Yu, J.R. Turner, Tight junction pore and leak pathways: a dynamic duo, Annu. Rev. Physiol. 73 (2011) 283–309.
[34] J.R. Turner, Intestinal mucosal barrier function in health and disease, Nat. Rev. Immunol. 9 (2009) 799–809.
[35] K. Sugano, M. Kansy, P. Artursson, A. Avdeef, S. Bendels, L. Di, G.F. Ecker, B. Faller, H. Fischer, G. Gerebtzoff, H. Lennernaes, F. Senner, Coexistence of passive and carrier-mediated processes in drug transport, Nat. Rev. Drug Discov. 9 (2010) 597–614.
[36] M.J. Mitchell, M.M. Billingsley, R.M. Haley, M.E. Wechsler, N.A. Peppas, R. Langer, Engineering precision nanoparticles for drug delivery, Nat. Rev. Drug Discov. 20 (2021) 101–124.
[37] L.J. Nugent, R.K. Jain, Extravascular diffusion in normal and neoplastic tissues, Cancer Res. 44 (1984) 238–244.
[38] A. Pluen, Y. Boucher, S. Ramanujan, T.D. McKee, T. Gohongi, E. di Tomaso, E. B. Brown, Y. Izumi, R.B. Campbell, D.A. Berk, R.K. Jain, Role of tumor-host interactions in interstitial diffusion of macromolecules: cranial vs. subcutaneous tumors, Proc. Natl. Acad. Sci. U. S. A. 98 (2001) 4628–4633.
[39] G.L. Rapaccini, A. Aliotta, M. Pompili, A. Grattagliano, M. Anti, B. Merlino, G. Gambassi, Gastric wall thickness in normal and neoplastic subjects - a prospective-study performed by abdominal ultrasound, Gastrointest. Radiol. 13 (1988) 197–199.
[40] G.J. Tortora, B.H. Derrickson, Principles of Anatomy and Physiology, 16 ed., John Wiley & Sons, 2020.
[41] N. Hoshyar, S. Gray, H. Han, G. Bao, The effect of nanoparticle size on in vivo pharmacokinetics and cellular interaction, Nanomedicine 11 (2016) 673–692.
[42] M. Cooley, A. Sarode, M. Hoore, D.A. Fedosov, S. Mitragotri, A.S. Gupta, Influence of particle size and shape on their margination and wall-adhesion: implications in drug delivery vehicle design across nano-to-micro scale, Nanoscale 10 (2018) 15350–15364.
[43] H. Soo Choi, W. Liu, P. Misra, E. Tanaka, J.P. Zimmer, B. Itty Ipe, M.G. Bawendi, J.V. Frangioni, Renal clearance of quantum dots, Nat. Biotechnol. 25 (2007) 1165–1170.
[44] M. Yu, J. Zheng, Clearance pathways and tumor targeting of imaging nanoparticles, ACS Nano 9 (2015) 6655–6674.
[45] R.K. Jain, Transport of molecules across tumor vasculature, Cancer Metastasis Rev. 6 (1987) 559–593.
[46] W. Whyte, D. Goswami, S.X. Wang, Y.L. Fan, N.A. Ward, R.E. Levey, R. Beatty, S. T. Robinson, D. Sheppard, R. O'Connor, D.S. Monahan, L. Trask, K.L. Mendez, C. E. Varela, M.A. Horvath, R. Wylie, J. O'Dwyer, D.A. Domingo-Lopez, A. S. Rothman, G.P. Duffy, E.B. Dolan, E.T. Roche, Dynamic actuation enhances transport and extends therapeutic lifespan in an implantable drug delivery platform, Nat. Commun. 13 (2022) 4496.
[47] O. Veiseh, J.C. Doloff, M.L. Ma, A.J. Vegas, H.H. Tam, A.R. Bader, J. Li, E. Langan, J. Wyckoff, W.S. Loo, S. Jhunjhunwala, A. Chiu, S. Siebert, K. Tang, J. Hollister-Lock, S. Aresta-Dasilva, M. Bochenek, J. Mendoza-Elias, Y. Wang, M. Qi, D.M. Lavin, M. Chen, N. Dholakia, R. Thakrar, I. Lacík, G.C. Weir, J. Oberholzer, D.L. Greiner, R. Langer, D.G. Anderson, Size-and shape-dependent foreign body immune response to materials implanted in rodents and non-human primates, Nat. Mater. 14 (2015) 643–651.
[48] R. Junghans, Finally! The Brambell receptor (FcRB) mediator of transmission of immunity and protection from catabolism for IgG, Immunol. Res. 16 (1997) 29–57.
[49] W. Wang, E. Wang, J. Balthasar, Monoclonal antibody pharmacokinetics and pharmacodynamics, Clin. Pharmacol. Ther. (St. Louis, MO, U. S.) 84 (2008) 548–558.
[50] A.S.A. Lila, H. Kiwada, T. Ishida, The accelerated blood clearance (ABC) phenomenon: clinical challenge and approaches to manage, J. Control. Release 172 (2013) 38–47.
[51] T.N. Nagaraja, P. Patel, M. Gorski, P.D. Gorevic, C.S. Patlak, J.D. Fenstermacher, In normal rat, intraventricularly administered insulin-like growth factor-1 is rapidly cleared from CSF with limited distribution into brain, Cerebrospinal Fluid Res. 2 (2005) 1–15.
[52] N.H. Greig, W.R. Fredericks, H.W. Holloway, T.T. Soncrant, S.I. Rapoport, Delivery of human interferon-alpha to brain by transient osmotic blood-brain barrier modification in the rat, J. Pharmacol. Exp. Ther. 245 (1988) 581–586.
[53] Y. Zhang, W.M. Pardridge, Mediated efflux of IgG molecules from brain to blood across the blood–brain barrier, J. Neuroimmunol. 114 (2001) 168–172.
[54] X. Huang, C.S. Brazel, On the importance and mechanisms of burst release in matrix-controlled drug delivery systems, J. Control. Release 73 (2001) 121–136.
[55] X.G. Lu, L. Miao, W.T. Gao, Z.Q. Chen, K.J. McHugh, Y.H. Sun, Z. Tochka, S. Tomasic, K. Sadtler, A. Hyacinthe, Y.X. Huang, T. Graf, Q.Y. Hu, M. Sarmadi, R. Langer, D.G. Anderson, A. Jaklenec, Engineered PLGA microparticles for long-term, pulsatile release of STING agonist for cancer immunotherapy, Sci. Transl. Med. 12 (2020).
[56] K.J. McHugh, T.D. Nguyen, A.R. Linehan, D. Yang, A.M. Behrens, S. Rose, Z. L. Tochka, S.Y. Tzeng, J.J. Norman, A.C. Anselmo, X. Xu, S. Tomasic, M.A. Taylor, J. Lu, R. Guarecuco, R. Langer, A. Jaklenec, Fabrication of fillable microparticles and other complex 3D microstructures, Science 357 (2017) 1138-+.
[57] N. Huebsch, C.J. Kearney, X.H. Zhao, J. Kim, C.A. Cezar, Z.G. Suo, D.J. Mooney, Ultrasound-triggered disruption and self-healing of reversibly cross-linked hydrogels for drug delivery and enhanced chemotherapy, Proc. Natl. Acad. Sci. U. S. A. 111 (2014) 9762–9767.
[58] J. Conde, N. Oliva, Y. Zhang, N. Artzi, Local triple-combination therapy results in tumour regression and prevents recurrence in a colon cancer model, Nat. Mater. 15 (2016) 1128–+.
[59] C. Dagdeviren, K.B. Ramadi, P. Joe, K. Spencer, H.N. Schwerdt, H. Shimazu, S. Delcasso, K.I. Amemori, C. Nunez-Lopez, A.M. Graybiel, M.J. Cima, R. Langer, Miniaturized neural system for chronic, local intracerebral drug delivery, Sci. Transl. Med. 10 (2018).
[60] P. Trojanowski, B. Jarosz, D. Szczepanek, The diagnostic quality of needle brain biopsy specimens obtained with different sampling methods–experimental study, Sci. Rep. 9 (2019) 1–7.

[61] T. Ben-Menachem, G.A. Decker, D.S. Early, J. Evans, R.D. Fanelli, D.A. Fisher, L. Fisher, N. Fukami, J.H. Hwang, S.O. Ikenberry, Adverse events of upper GI endoscopy, Gastrointest. Endosc. 76 (2012) 707–718.
[62] P. Haas, C. Falkner-Radler, B. Wimpissinger, M. Malina, S. Binder, Needle size in intravitreal injections–pain evaluation of a randomized clinical trial, Acta Ophthalmol. 94 (2016) 198–202.
[63] R.R. Lonser, M. Sarntinoranont, P.F. Morrison, E.H. Oldfield, Convection-enhanced delivery to the central nervous system, J. Neurosurg. 122 (2015) 697–706.
[64] A.M. Mehta, A.M. Sonabend, J.N. Bruce, Convection-enhanced delivery, Neurotherapeutics 14 (2017) 358–371.
[65] A.P. Kells, P. Hadaczek, D.L. Yin, J. Bringas, V. Varenika, J. Forsayeth, K. S. Bankiewicz, Efficient gene therapy-based method for the delivery of therapeutics to primate cortex, Proc. Natl. Acad. Sci. U. S. A. 106 (2009) 2407–2411.
[66] K. Negron, G. Kwak, H. Wang, H.L. Li, Y.T. Huang, S.W. Chen, B. Tyler, C. G. Eberhart, J. Hanes, J.S. Suk, A highly translatable dual-arm local delivery strategy to achieve widespread therapeutic coverage in healthy and tumor-bearing brain tissues, Small 19 (2023).
[67] K.S. Bankiewicz, J.L. Eberling, M. Kohutnicka, W. Jagust, P. Pivirotto, J. Bringas, J. Cunningham, T.F. Budinger, J. Harvey-White, Convection-enhanced delivery of AAV vector in parkinsonian monkeys; In vivo detection of gene expression and restoration of dopaminergic function using pro-drug approach, Exp. Neurol. 164 (2000) 2–14.
[68] K.S. Bankiewicz, V. Sudhakar, L. Samaranch, W. San Sebastian, J. Bringas, J. Forsayeth, AAV viral vector delivery to the brain by shape-conforming MR-guided infusions, J. Control. Release 240 (2016) 434–442.
[69] N. Dube, J.Y. Shu, H. Dong, J.W. Seo, E. Ingham, A. Kheirolomoom, P.Y. Chen, J. Forsayeth, K. Bankiewicz, K.W. Ferrara, T. Xu, Evaluation of doxorubicin-loaded 3-Helix micelles as Nanocarriers, Biomacromolecules 14 (2013) 3697–3705.
[70] M.T. Krauze, R. Saito, C. Noble, M. Tamas, J. Bringas, J.W. Park, M.S. Berger, K. Bankiewicz, Reflux-free cannula for convection-enhanced high-speed delivery of therapeutic agents - technical note, J. Neurosurg. 103 (2005) 923–929.
[71] R. Saito, J.R. Bringas, T.R. McKnight, M.F. Wendland, C. Mamot, D. C. Drummond, D.B. Kirpotin, J.W. Park, M.S. Berger, K.S. Bankiewicz, Distribution of liposomes into brain and rat brain tumor models by convection-enhanced delivery monitored with magnetic resonance imaging, Cancer Res. 64 (2004) 2572–2579.
[72] W. Mok, T. Stylianopoulos, Y. Boucher, R.K. Jain, Mathematical modeling of herpes simplex virus distribution in solid tumors: implications for cancer gene therapy, Clin. Cancer Res. 15 (2009) 2352–2360.
[73] M. Cotler, E.B. Rousseau, K.B. Ramadi, O.S. Fang, A.M. Graybiel, R. Langer, M. J. Cima, Steerable microinvasive probes for localized drug delivery to deep tissue, Small 15 (2019).
[74] K.B. Ramadi, C. Dagdeviren, K.C. Spencer, P. Joe, M. Cotler, E. Rousseau, C. Nunez-Lopez, A.M. Graybiel, R. Langer, M.J. Cima, Focal, remote-controlled, chronic chemical modulation of brain microstructures, Proc. Natl. Acad. Sci. U. S. A. 115 (2018) 7254–7259.
[75] E. Wembacher-Schroeder, N. Kerstein, E.D. Bander, N. Pandit-Taskar, R. Thomson, M.M. Souweidane, Evaluation of a patient-specific algorithm for predicting distribution for convection-enhanced drug delivery into the brainstem of patients with diffuse intrinsic pontine glioma, J. Neurosurg.-Pediatr. 28 (2020) 34–42.
[76] J.H. Sampson, R. Raghavan, M.L. Brady, J.M. Provenzale, J.E. Herndon, D. Croteau, A.H. Friedman, D.A. Reardon, R.E. Coleman, T. Wong, D.D. Bigner, I. Pastan, M.I. Rodriguez-Ponce, P. Tanner, R. Puri, C. Pedain, Clinical utility of a patient-specific algorithm for simulating intracerebral drug infusions, Neuro-Oncology 9 (2007) 343–353.
[77] K.B. Ramadi, A. Bashyam, C.J. Frangieh, E.B. Rousseau, M.J. Cotler, R. Langer, A. M. Graybiel, M.J. Cima, Computationally guided intracerebral drug delivery via chronically implanted microdevices, Cell Rep. 31 (2020).
[78] A.S. Fargnoli, M.G. Katz, R.D. Williams, A.P. Kendle, N. Steuerwald, C.R. Bridges, Liquid jet delivery method featuring S100A1 gene therapy in the rodent model following acute myocardial infarction, Gene Ther. 23 (2016) 151–157.
[79] M. Kaya, B. Ahishali, Basic physiology of the blood-brain barrier in health and disease: a brief overview, Tissue Barri. 9 (2021) 1840913.
[80] C.A. Loehry, A.T.R. Axon, P.J. Hilton, R.C. Hider, B. Creamer, Permeability of the small intestine to substances of different molecular weight, Gut 11 (1970) 466–470.
[81] J.D. Bos, M.M. Meinardi, The 500 Dalton rule for the skin penetration of chemical compounds and drugs, Experimen. Dermatol.: Viewpoint 9 (2000) 165–169.
[82] S.P. Small, Preventing sciatic nerve injury from intramuscular injections: literature review, J. Adv. Nurs. 47 (2004) 287–296.
[83] F. Kroschinsky, F. Stölzel, S. von Bonin, G. Beutel, M. Kochanek, M. Kiehl, P. Schellongowski, O., Intensive care hematological, new drugs, new toxicities: severe side effects of modern targeted and immunotherapy of cancer and their management, Crit. Care 21 (2017).
[84] A. Abramson, A.R. Kirtane, Y.H. Shi, G. Zhong, J.E. Collins, S. Tamang, K. Ishida, A. Hayward, J. Wainer, N.U. Rajesh, X.Y. Lu, Y. Gao, P. Karandikar, C.Y. Tang, A. Lopes, A. Wahane, D. Reker, M.R. Frederiksen, B. Jensen, R. Langer, G. Traverso, Oral mRNA delivery using capsule-mediated gastrointestinal tissue injections, Matter 5 (2022) 975–987.
[85] E.E. Engwerda, E.J. Abbink, C.J. Tack, B.E. De Galan, Improved pharmacokinetic and pharmacodynamic profile of rapid-acting insulin using needle-free jet injection technology, Diabetes Care 34 (2011) 1804–1808.
[86] K. Aran, M. Chooljian, J. Paredes, M. Rafi, K. Lee, A.Y. Kim, J. An, J.F. Yau, H. Chum, I. Conboy, N. Murthy, D. Liepmann, An oral microjet vaccination system elicits antibody production in rabbits, Sci. Transl. Med. 9 (2017) eaaf6413.
[87] M. Hashim, R. Korupolu, B. Syed, K. Horlen, S. Beraki, P. Karamchedu, A. K. Dhalla, R. Ruffy, M. Imran, Jejunal wall delivery of insulin via an ingestible capsule in anesthetized swine—a pharmacokinetic and pharmacodynamic study, Pharmacol. Res. Perspect. 7 (2019) e00522.
[88] A.K. Dhalla, Z. Al-Shamsie, S. Beraki, A. Dasari, L.C. Fung, L. Fusaro, A. Garapaty, B. Gutierrez, D. Gratta, M. Hashim, K. Horlen, P. Karamchedu, R. Korupolu, E. Liang, C. Ong, Z. Owyang, V. Salgotra, S. Sharma, B. Syed, M. Syed, A.T. Vo, R. Abdul-Wahab, A. Wasi, A. Yamaguchi, S.E. Yen, M. Imran, A robotic pill for oral delivery of biotherapeutics: safety, tolerability, and performance in healthy subjects, Drug Deliv. Transl. Res. 12 (2022) 294–305.
[89] R. Ghanim, A. Kaushik, J. Park, A. Abramson, Communication protocols integrating wearables, ingestibles, and implantables for closed-loop therapies, Device 1 (2023).
[90] A.Z. Fu, Y. Qiu, L. Radican, Impact of fear of insulin or fear of injection on treatment outcomes of patients with diabetes, Curr. Med. Res. Opin. 25 (2009) 1413–1420.
[91] M.R. Prausnitz, R. Langer, Transdermal drug delivery, Nat. Biotechnol. 26 (2008) 1261–1268.
[92] R.O. Potts, M.L. Francoeur, The influence of stratum corneum morphology on water permeability, J. Investig. Dermatol. 96 (1991) 495–499.
[93] D.A. Schwindt, K.P. Wilhelm, H.I. Maibach, Water diffusion characteristics of human stratum corneum at different anatomical sites in vivo, J. Investig. Dermatol. 111 (1998) 385–389.
[94] S. Mitragotri, In situ determination of partition and diffusion coefficients in the lipid bilayers of stratum corneum, Pharm. Res. 17 (2000) 1026.
[95] J. Niu, Y. Chu, Y.-F. Huang, Y.-S. Chong, Z.-H. Jiang, Z.-W. Mao, L.-H. Peng, J.-Q. Gao, Transdermal gene delivery by functional peptide-conjugated cationic gold nanoparticle reverses the progression and metastasis of cutaneous melanoma, ACS Appl. Mater. Interfaces 9 (2017) 9388–9401.
[96] A.W. Pryde, E.P. Pendergrass, An experimental study of the Gastric Wall thickness at the site of peristalsis in dogs, Radiology 62 (1954) 559–568.
[97] A. Sharma, J.-G. Kwak, K.W. Kolewe, J.D. Schiffman, N.S. Forbes, J. Lee, In vitro reconstitution of an intestinal mucus layer shows that cations and pH control the pore structure that regulates its permeability and barrier function, ACS Appl. Bio Mater. 3 (2020) 2897–2909.
[98] K. Whitehead, N. Karr, S. Mitragotri, Safe and effective permeation enhancers for oral drug delivery, Pharm. Res. 25 (2008) 1782–1788.
[99] S.S. Srinivasan, A. Alshareef, A.V. Hwang, Z.L. Kang, J. Kuosmanen, K. Ishida, J. Jenkins, S. Liu, W.A.M. Madani, J. Lennerz, A. Hayward, J. Morimoto, N. Fitzgerald, R. Langer, G. Traverso, RoboCap: robotic mucus-clearing capsule for enhanced drug delivery in the gastrointestinal tract, Sci. Robot. 7 (2022).
[100] W.M. Pardridge, Drug transport across the blood-brain barrier, J. Cereb. Blood Flow Metab. 32 (2012) 1959–1972.
[101] Y.J. Yu, Y. Zhang, M. Kenrick, K. Hoyte, W. Luk, Y.M. Lu, J. Atwal, J.M. Elliott, S. Prabhu, R.J. Watts, M.S. Dennis, Boosting brain uptake of a therapeutic antibody by reducing its affinity for a transcytosis target, Sci. Transl. Med. 3 (2011).
[102] Y. Zhang, W.M. Pardridge, Rapid transferrin efflux from brain to blood across the blood–brain barrier, J. Neurochem. 76 (2001) 1597–1600.
[103] P.R. Cooper, G.J. Ciambrone, C.M. Kliwinski, E. Maze, L. Johnson, Q. Li, Y. Feng, P.J. Hornby, Efflux of monoclonal antibodies from rat brain by neonatal fc receptor, FcRn, Brain Res. 1534 (2013) 13–21.
[104] W.M. Pardridge, Drug transport in brain via the cerebrospinal fluid, Fluid. Barri. CNS 8 (2011) 1–4.
[105] B. Van Deurs, J. Koehler, Tight junctions in the choroid plexus epithelium. A freeze-fracture study including complementary replicas, J. Cell Biol. 80 (1979) 662–673.
[106] L. Sakka, G. Coll, J. Chazal, Anatomy and physiology of cerebrospinal fluid, Eur. Ann. Otorhinolaryngol. Head Neck Dis. 128 (2011) 309–316.
[107] M. Mak, L. Fung, J.F. Strasser, W.M. Saltzman, Distribution of drugs following controlled delivery to the brain interstitium, J. Neuro-Oncol. 26 (1995) 91–102.
[108] A. Billiau, H. Heremans, D. Ververken, J. Van Damme, H. Carton, P. De Somer, Tissue distribution of human interferons after exogenous administration in rabbits, monkeys, and mice, Arch. Virol. 68 (1981) 19–25.
[109] R.K. Jain, L.T. Baxter, Mechanisms of heterogeneous distribution of monoclonal-antibodies and other macromolecules in tumors - significance of elevated interstitial pressure, Cancer Res. 48 (1988) 7022–7032.
[110] M. Hockel, P. Vaupel, Tumor hypoxia: definitions and current clinical, biologic, and molecular aspects, J. Natl. Cancer Inst. 93 (2001) 266–276.
[111] D. Liao, R.S. Johnson, Hypoxia: a key regulator of angiogenesis in cancer, Cancer Metastasis Rev. 26 (2007) 281–290.
[112] K. Urbańska, J. Sokołowska, M. Szmidt, P. Sysa, Glioblastoma multiforme–an overview, Contemp. Oncol./Współczesna Onkologia 18 (2014) 307–312.
[113] F.C. Detterbeck, D.J. Boffa, A.W. Kim, L.T. Tanoue, The eighth edition lung cancer stage classification, Chest 151 (2017) 193–203.
[114] J.E. Moulder, S. Rockwell, Hypoxic fractions of solid tumors: experimental techniques, methods of analysis, and a survey of existing data, Int. J. Radiat. Oncol. Biol. Phys. 10 (1984) 695–712.
[115] X.-F. Li, S. Carlin, M. Urano, J. Russell, C.C. Ling, J.A. O'Donoghue, Visualization of hypoxia in microscopic tumors by immunofluorescent microscopy, Cancer Res. 67 (2007) 7646–7653.

[116] L.T. Baxter, R.K. Jain, Transport of fluid and macromolecules in tumors. II. Role of heterogeneous perfusion and lymphatics, Microvasc. Res. 40 (1990) 246–263.
[117] M.J. Ernsting, M. Murakami, A. Roy, S.-D. Li, Factors controlling the pharmacokinetics, biodistribution and intratumoral penetration of nanoparticles, J. Control. Release 172 (2013) 782–794.
[118] A.I. Minchinton, I.F. Tannock, Drug penetration in solid tumours, Nat. Rev. Cancer 6 (2006) 583–592.
[119] L.H. Hartwell, M.B. Kastan, Cell cycle control and cancer, Science 266 (1994) 1821–1828.
[120] A. Kanesa-thasan, P. Tyler, J. Nicolai, D. Procissi, J. Chen, R. Lewandowski, R. Salem, A. Larson, R. Omary, Comparison of image-guided intratumoral versus intravenous delivery of therapeutic nanoparticles for the treatment of hepatocellular carcinoma, J. Vasc. Interv. Radiol. 24 (2013) S142.
[121] W.J. Bodell, A.P. Bodell, D.D. Giannini, Levels and distribution of BCNU in GBM tumors following intratumoral injection of DTI-015 (BCNU-ethanol), Neuro-Oncology 9 (2007) 12–19.
[122] N.M. Muñoz, M. Williams, K. Dixon, C. Dupuis, A. McWatters, R. Avritscher, S. Z. Manrique, K. McHugh, R. Murthy, A. Tam, Influence of injection technique, drug formulation and tumor microenvironment on intratumoral immunotherapy delivery and efficacy, J. Immunother. Cancer 9 (2021).
[123] Y. Wang, J.K. Hu, A. Krol, Y.-P. Li, C.-Y. Li, F. Yuan, Systemic dissemination of viral vectors during intratumoral injection, Mol. Cancer Ther. 2 (2003) 1233–1242.
[124] W.J. Polacheck, J.L. Charest, R.D. Kamm, Interstitial flow influences direction of tumor cell migration through competing mechanisms, Proc. Natl. Acad. Sci. 108 (2011) 11115–11120.
[125] G. Charras, E. Sahai, Physical influences of the extracellular environment on cell migration, Nat. Rev. Mol. Cell Biol. 15 (2014) 813–824.
[126] P.M. Treuting, S. Dintzis, K.S. Montine, Comparative Anatomy and Histology: A Mouse, Rat, and Human Atlas, Academic Press, 2017.
[127] W. Whyte, E.T. Roche, C.E. Varela, K. Mendez, S. Islam, H. O'Neill, F. Weafer, R. N. Shirazi, J.C. Weaver, N.V. Vasilyev, P.E. McHugh, B. Murphy, G.P. Duffy, C. J. Walsh, D.J. Mooney, Sustained release of targeted cardiac therapy with a replenishable implanted epicardial reservoir, nature, Biomed. Eng. 2 (2018) 416–428.
[128] C. Wu, Y.X. Zhang, Y.Y. Xu, L.Y. Long, X.F. Hu, J.Y. Zhang, Y.B. Wang, Injectable polyaniline nanorods/alginate hydrogel with AAV9-mediated VEGF overexpression for myocardial infarction treatment, Biomaterials 296 (2023).
[129] T. Bejerano, S. Etzion, S. Elyagon, Y. Etzion, S. Cohen, Nanoparticle delivery of miRNA-21 mimic to cardiac macrophages improves myocardial remodeling after myocardial infarction, Nano Lett. 18 (2018) 5885–5891.
[130] D. Hou, E.A.-S. Youssef, T.J. Brinton, P. Zhang, P. Rogers, E.T. Price, A.C. Yeung, B.H. Johnstone, P.G. Yock, K.L. March, Radiolabeled cell distribution after intramyocardial, intracoronary, and interstitial retrograde coronary venous delivery: implications for current clinical trials, Circulation 112 (2005). I-150-I-156.
[131] P.M. Grossman, Z. Han, M. Palasis, J.J. Barry, R.J. Lederman, Incomplete retention after direct myocardial injection, Catheter. Cardiovasc. Interv. 55 (2002) 392–397.
[132] A.N. Steele, M.J. Paulsen, H. Wang, L.M. Stapleton, H.J. Lucian, A. Eskandari, C. E. Hironaka, J.M. Farry, S.W. Baker, A.D. Thakore, K.J. Jaatinen, Y. Tada, M. J. Hollander, K.M. Williams, A.J. Seymour, K.P. Totherow, A.C. Yu, J.R. Cochran, E.A. Appel, Y.J. Woo, Multi-phase catheter-injectable hydrogel enables dual-stage protein-engineered cytokine release to mitigate adverse left ventricular remodeling following myocardial infarction in a small animal model and a large animal model, Cytokine 127 (2020).
[133] T.D. Johnson, K.L. Christman, Injectable hydrogel therapies and their delivery strategies for treating myocardial infarction, Expert Opin. Drug Deliv. 10 (2013) 59–72.
[134] J.L. Ifkovits, E. Tous, M. Minakawa, M. Morita, J.D. Robb, K.J. Koomalsingh, J. H. Gorman III, R.C. Gorman, J.A. Burdick, Injectable hydrogel properties influence infarct expansion and extent of postinfarction left ventricular remodeling in an ovine model, Proc. Natl. Acad. Sci. 107 (2010) 11507–11512.
[135] T. Kofidis, J.L. de Bruin, G. Hoyt, D.R. Lebl, M. Tanaka, T. Yamane, C.-P. Chang, R.C. Robbins, Injectable bioartificial myocardial tissue for large-scale intramural cell transfer and functional recovery of injured heart muscle, J. Thorac. Cardiovasc. Surg. 128 (2004) 571–578.
[136] J.M. Singelyn, P. Sundaramurthy, T.D. Johnson, P.J. Schup-Magoffin, D.P. Hu, D. M. Faulk, J. Wang, K.M. Mayle, K. Bartels, M. Salvatore, A.M. Kinsey, A. N. DeMaria, N. Dib, K.L. Christman, Catheter-deliverable hydrogel derived from Decellularized ventricular extracellular matrix increases endogenous cardiomyocytes and preserves cardiac function post-myocardial infarction, J. Am. Coll. Cardiol. 59 (2012) 751–763.
[137] L. Stapleton, Y. Zhu, Y.-P.J. Woo, E. Appel, Engineered biomaterials for heart disease, Curr. Opin. Biotechnol. 66 (2020) 246–254.
[138] P. Raake, G. von Degenfeld, R. Hinkel, R. Vachenauer, T. Sandner, S. Beller, M. Andrees, C. Kupatt, G. Schuler, P. Boekstegers, Myocardial gene transfer by selective pressure-regulated retroinfusion of coronary veins: comparison with surgical and percutaneous intramyocardial gene delivery, J. Am. Coll. Cardiol. 44 (2004) 1124–1129.
[139] M.J. Doughty, M.L. Zaman, Human corneal thickness and its impact on intraocular pressure measures: a review and meta-analysis approach, Surv. Ophthalmol. 44 (2000) 367–408.
[140] Y.C. Kim, B. Chiang, X. Wu, M.R. Prausnitz, Ocular delivery of macromolecules, J. Control. Release 190 (2014) 172–181.
[141] K.-M. Hämäläinen, K. Kananen, S. Auriola, K. Kontturi, A. Urtti, Characterization of paracellular and aqueous penetration routes in cornea, conjunctiva, and sclera, Invest. Ophthalmol. Vis. Sci. 38 (1997) 627–634.
[142] A. Urtti, Challenges and obstacles of ocular pharmacokinetics and drug delivery, Adv. Drug Deliv. Rev. 58 (2006) 1131–1135.
[143] Y.C. Kim, M.D. Shin, S.F. Hackett, H.T. Hsueh, R.L.E. Silva, A. Date, H. Han, B. J. Kim, A. Xiao, Y. Kim, L. Ogunnaike, N.M. Anders, A. Hemingway, P. He, A. S. Jun, P.J. McDonnell, C. Eberhart, I. Pitha, D.J. Zack, P.A. Campochiaro, J. Hanes, L.M. Ensign, Gelling hypotonic polymer solution for extended topical drug delivery to the eye, nature, Biomed. Eng. 4 (2020), 1053-+.
[144] B. Chiang, J.H. Jung, M.R. Prausnitz, The suprachoroidal space as a route of administration to the posterior segment of the eye, Adv. Drug Deliv. Rev. 126 (2018) 58–66.
[145] J.H. Jung, B. Chiang, H.E. Grossniklaus, M.R. Prausnitz, Ocular drug delivery targeted by iontophoresis in the suprachoroidal space using a microneedle, J. Control. Release 277 (2018) 14–22.
[146] G.D. Chitnis, M.K.S. Verma, J. Lamazouade, M. Gonzalez-Andrades, A. KisukYan, P.A. Dergham, B.E. Jones, A. Mead, Z.X. Cruzat, K. Tong, A. Martyn, N. Solanki, J. M. Karp Landon-Brace, A resistance-sensing mechanical injector for the precise delivery of liquids to target tissue, Nat. Biomed. Eng. 3 (2019) 621–631.
[147] J.M. Anderson, A. Rodriguez, D.T. Chang, Foreign body reaction to biomaterials, Semin. Immunol. 20 (2008) 86–100.
[148] W.K. Ward, A review of the foreign-body response to subcutaneously-implanted devices: the role of macrophages and cytokines in biofouling and fibrosis, J. Diabetes Sci. Technol. 2 (2008) 768–777.
[149] A.A. Sharkawy, B. Klitzman, G.A. Truskey, W.M. Reichert, Engineering the tissue which encapsulates subcutaneous implants. I. Diffusion properties, J. Biomed. Mater. Res.: Off. J. Soc. Biomater. Japan. Soc. Biomater. 37 (1997) 401–412.
[150] L.S. Kumosa, T.L. Routh, J.T. Lin, J.Y. Lucisano, D.A. Gough, Permeability of subcutaneous tissues surrounding long-term implants to oxygen, Biomaterials 35 (2014) 8287–8296.
[151] O. Veiseh, A.J. Vegas, Domesticating the foreign body response: recent advances and applications, Adv. Drug Deliv. Rev. 144 (2019) 148–161.
[152] A.J. Vegas, O. Veiseh, J.C. Doloff, M.L. Ma, H.H. Tam, K. Bratlie, J. Li, A.R. Bader, E. Langan, K. Olejnik, P. Fenton, J.W. Kang, J. Hollister-Locke, M.A. Bochenek, A. Chiu, S. Siebert, K. Tang, S. Jhunjhunwala, S. Aresta-Dasilva, N. Dholakia, R. Thakrar, T. Vietti, M. Chen, J. Cohen, K. Siniakowicz, M.R.G. Qi, J. McGarrigle, S. Lyle, D.M. Harlan, D.L. Greiner, J. Oberholzer, G.C. Weir, R. Langer, D. G. Anderson, Combinatorial hydrogel library enables identification of materials that mitigate the foreign body response in primates, Nat. Biotechnol. 34 (2016), 345-+.
[153] J.C. Doloff, O. Veiseh, R. de Mezerville, M. Sforza, T.A. Perry, J. Haupt, M. Jamiel, C. Chambers, A. Nash, S. Aghlara-Fotovat, J.L. Stelzel, S.J. Bauer, S.Y. Neshat, J. Hancock, N.A. Romero, Y.E. Hidalgo, I.M. Leiva, A.M. Munhoz, A. Bayat, B. M. Kinney, H.C. Hodges, R.N. Miranda, M.W. Clemens, R. Langer, The surface topography of silicone breast implants mediates the foreign body response in mice, rabbits and humans, Nat. Biomed. Eng. 5 (2021) 1115–1130.
[154] X. Xie, J.C. Doloff, V. Yesilyurt, A. Sadraei, J.J. McGarrigle, M. Commis, O. Veiseh, S. Farah, D. Isa, S. Ghanis, I. Joshis, A. Vegas, J. Li, W.H. Wang, A. Bader, H.H. Tam, J. Tao, H.J. Chen, B.R. Yang, K.A. Williamson, J. Oberholzers, R. Langer, D.G. Anderson, Reduction of measurement noise in a continuous glucose monitor by coating the sensor with a zwitterionic polymer, Nat. Biomed. Eng. 2 (2018) 894–906.
[155] E.B. Dolan, C.E. Varela, K. Mendez, W. Whyte, R.E. Levey, S.T. Robinson, E. Maye, J. O'Dwyer, R. Beatty, A. Rothman, Y. Fan, J. Hochstein, S.E. Rothenbucher, R. Wylie, J.R. Starr, M. Monaghan, P. Dockery, G.P. Duffy, E.T. Roche, An actuatable soft reservoir modulates host foreign body response, Sci. Robot. 4 (2019) eaax7043.
[156] P.N. Schlegel, H.S. Group, Efficacy and safety of histrelin subdermal implant in patients with advanced prostate cancer, J. Urol. 175 (2006) 1353–1358.
[157] E.D. Deeks, Histrelin: in advanced prostate cancer, Drugs 70 (2010) 623–630.
[158] D. Adams, A. Gonzalez-Duarte, W.D. O'Riordan, C.C. Yang, M. Ueda, A.V. Kristen, I. Tournev, H.H. Schmidt, T. Coelho, J.L. Berk, K.P. Lin, G. Vita, S. Attarian, V. Planté-Bordeneuve, M.M. Mezei, J.M. Campistol, J. Buades, T.H. Brannagan, B. J. Kim, J. Oh, Y. Parman, Y. Sekijima, P.N. Hawkins, S.D. Solomon, M. Polydefkis, P.J. Dyck, P.J. Gandhi, S. Goyal, J. Chen, A.L. Strahs, S.V. Nochur, M.T. Sweetser, P.P. Garg, A.K. Vaishnaw, J.A. Gollob, O.B. Suhr, Patisiran, an RNAi therapeutic, for hereditary transthyretin amyloidosis, N. Engl. J. Med. 379 (2018) 11–21.
[159] A. Akinc, M.A. Maier, M. Manoharan, K. Fitzgerald, M. Jayaraman, S. Barros, S. Ansell, X.Y. Du, M.J. Hope, T.D. Madden, B.L. Mui, S.C. Semple, Y.K. Tam, M. Ciufolini, D. Witzigmann, J.A. Kulkarni, R. van der Meel, P.R. Cullis, The Onpattro story and the clinical translation of nanomedicines containing nucleic acid-based drugs, Nat. Nanotechnol. 14 (2019) 1084–1087.
[160] I. Urits, D. Swanson, M.C. Swett, A. Patel, K. Berardino, A. Amgalan, A.A. Berger, H. Kassem, A.D. Kaye, O. Viswanath, A review of patisiran (ONPATTRO®) for the treatment of polyneuropathy in people with hereditary transthyretin amyloidosis, Neurol. Therapy 9 (2020) 301–315.
[161] S. Shetty, P.F. Lalor, D.H. Adams, Liver sinusoidal endothelial cells—gatekeepers of hepatic immunity, Nat. Rev. Gastroenterol. Hepatol. 15 (2018) 555–567.
[162] F.P. Polack, S.J. Thomas, N. Kitchin, J. Absalon, A. Gurtman, S. Lockhart, J. L. Perez, G.P. Marc, E.D. Moreira, C. Zerbini, R. Bailey, K.A. Swanson, S. Roychoudhury, K. Koury, P. Li, W.V. Kalina, D. Cooper, R.W. Frenck, L. L. Hammitt, O. Tureci, H. Nell, A. Schaefer, S. Unal, D.B. Tresnan, S. Mather, P. R. Dormitzer, U. Sahin, K.U. Jansen, W.C. Gruber, Safety and efficacy of the BNT162b2 mRNA Covid-19 vaccine, N. Engl. J. Med. 383 (2020) 2603–2615.

[163] L.R. Baden, H.M. El Sahly, B. Essink, K. Kotloff, S. Frey, R. Novak, D. Diemert, S. A. Spector, N. Rouphael, C.B. Creech, J. McGettigan, S. Khetan, N. Segall, J. Solis, A. Brosz, C. Fierro, H. Schwartz, K. Neuzil, L. Corey, P. Gilbert, H. Janes, D. Follmann, M. Marovich, J. Mascola, L. Polakowski, J. Ledgerwood, B. S. Graham, H. Bennett, R. Pajon, C. Knightly, B. Leav, W.P. Deng, H.H. Zhou, S. Han, M. Ivarsson, J. Miller, T. Zaks, Efficacy and safety of the mRNA-1273 SARS-CoV-2 vaccine, N. Engl. J. Med. 384 (2021) 403–416.
[164] F. Liang, G. Lindgren, A. Lin, E.A. Thompson, S. Ols, J. Röhss, S. John, K. Hassett, O. Yuzhakov, K. Bahl, L.A. Brito, H. Salter, G. Ciaramella, K. Loré, Efficient targeting and activation of antigen presenting cells in vivo after modified mRNA vaccine Administration in Rhesus Macaques, Mol. Ther. 25 (2017) 2635–2647.
[165] Y.C. Barenholz, Doxil®—the first FDA-approved nano-drug: lessons learned, J. Control. Release 160 (2012) 117–134.
[166] A.E. Green, P.G. Rose, Pegylated liposomal doxorubicin in ovarian cancer, Int. J. Nanomedicine 1 (2006) 229.
[167] H. Lee, C. Song, Y.S. Hong, M. Kim, H.R. Cho, T. Kang, K. Shin, S.H. Choi, T. Hyeon, D.-H. Kim, Wearable/disposable sweat-based glucose monitoring device with multistage transdermal drug delivery module, Sci. Adv. 3 (2017) e1601314.
[168] A. Abramson, E. Caffarel-Salvador, V. Soares, D. Minahan, R.Y. Tian, X.Y. Lu, D. Dellal, Y. Gao, S. Kim, J. Wainer, J. Collins, S. Tamang, A. Hayward, T. Yoshitake, H.C. Lee, J. Fujimoto, J. Fels, M.R. Frederiksen, U. Rahbek, N. Roxhed, R. Langer, G. Traverso, A luminal unfolding microneedle injector for oral delivery of macromolecules, Nat. Med. 25 (2019) 1512–+.
[169] N.C. Hogan, A.J. Taberner, L.A. Jones, I.W. Hunter, Needle-free delivery of macromolecules through the skin using controllable jet injectors, Expert Opin. Drug Deliv. 12 (2015) 1637–1648.
[170] G. Glenn, R. Kenney, Mass vaccination: solutions in the skin, in: Mass Vaccination: Global Aspects—Progress and Obstacles, 2006, pp. 247–268.
[171] S.J. Farr, B. Boyd, P. Bridges, L.S. Linn, Using Needle-Free Injectors for Parenteral Delivery of Proteins, Protein Formulation and Delivery, CRC Press, 2007, pp. 273–302.
[172] Y. Michinaka, S. Mitragotri, Delivery of polymeric particles into skin using needle-free liquid jet injectors, J. Control. Release 153 (2011) 249–254.
[173] O. Shpilberg, C. Jackisch, Subcutaneous administration of rituximab (MabThera) and trastuzumab (Herceptin) using hyaluronidase, Br. J. Cancer 109 (2013) 1556–1561.
[174] L. Bolondi, M. Bortolotti, V. Santi, T. Calletti, S. Gaiani, G. Labò, Measurement of gastric emptying time by real-time ultrasonography, Gastroenterology 89 (1985) 752–759.
[175] A. Fargnoli, M. Katz, R. Williams, K. Margulies, C.R. Bridges, A needleless liquid jet injection delivery method for cardiac gene therapy: a comparative evaluation versus standard routes of delivery reveals enhanced therapeutic retention and cardiac specific gene expression, J. Cardiovasc. Transl. Res. 7 (2014) 756–767.
[176] T. Gopesh, J.H. Wen, D. Santiago-Dieppa, B.A. Yan, J.S. Pannell, A. Khalessi, A. Norbash, J. Friend, Soft robotic steerable microcatheter for the endovascular treatment of cerebral disorders, Sci. Robot. 6 (2021).
[177] M.-H. Ling, M.-C. Chen, Dissolving polymer microneedle patches for rapid and efficient transdermal delivery of insulin to diabetic rats, Acta Biomater. 9 (2013) 8952–8961.
[178] K.T.M. Tran, T.D. Gavitt, N.J. Farrell, E.J. Curry, A.B. Mara, A. Patel, L. Brown, S. Kilpatrick, R. Piotrowska, N. Mishra, S.M. Szczepanek, T.D. Nguyen, Transdermal microneedles for the programmable burst release of multiple vaccine payloads, nature, Biomed. Eng. 5 (2021) 998–+.
[179] W. Li, J.Y. Chen, R.N. Terry, J. Tang, A. Romanyuk, S.P. Schwendeman, M. R. Prausnitz, Core-shell microneedle patch for six-month controlled-release contraceptive delivery, J. Control. Release 347 (2022) 489–499.
[180] W. Li, R.N. Terry, J. Tang, M.R. Feng, S.P. Schwendeman, M.R. Prausnitz, Rapidly separable microneedle patch for the sustained release of a contraceptive, Nat. Biomed. Eng. 3 (2019) 220–229.
[181] S. Babaee, S. Pajovic, A.R. Kirtane, J.Y. Shi, E. Caffarel-Salvador, K. Hess, J. E. Collins, S. Tamang, A.V. Wahane, A.M. Hayward, H. Mazdiyasni, R. Langer, G. Traverso, Temperature-responsive biometamaterials for gastrointestinal applications, Sci. Transl. Med. 11 (2019) eaau8581.
[182] S. Babaee, Y.C. Shi, S. Abbasalizadeh, S. Tamang, K. Hess, J.E. Collins, K. Ishida, A. Lopes, M. Williams, M. Albaghdadi, A.M. Hayward, G. Traverso, Kirigami-inspired stents for sustained local delivery of therapeutics, Nat. Mater. 20 (2021) 1085–1092.
[183] S.X. Huang, D. Lei, Q. Yang, Y. Yang, C.Y. Jiang, H.P. Shi, B. Qian, Q. Long, W. Y. Chen, Y.M. Chen, L. Zhu, W.J. Yang, L. Wang, W.X. Hai, Q. Zhao, Z.W. You, X. F. Ye, A perfusable, multifunctional epicardial device improves cardiac function and tissue repair, Nat. Med. 27 (2021) 480–490.
[184] H.P. Shi, T. Xue, Y. Yang, C.Y. Jiang, S.X. Huang, Q. Yang, D. Lei, Z.W. You, T. Jin, F. Wu, Q. Zhao, X.F. Ye, Microneedle-mediated gene delivery for the treatment of ischemic myocardial disease, Sci. Adv. 6 (2020) eaaz3621.
[185] J.N. Tang, J.Q. Wang, K. Huang, Y.Q. Ye, T. Su, L. Qiao, M.T. Hensley, T. G. Caranasos, J.Y. Zhang, Z. Gu, K. Cheng, Cardiac cell-integrated microneedle patch for treating myocardial infarction, Sci. Adv. 4 (2018).
[186] J.H. Traverse, T.D. Henry, N. Dib, A.N. Patel, C. Pepine, G.L. Schaer, J. A. DeQuach, A.M. Kinsey, P. Chamberlin, K.L. Christman, First-in-man study of a cardiac extracellular matrix hydrogel in early and late myocardial infarction patients, Basic to Translat. Sci. 4 (2019) 659–669.
[187] D. Bejleri, B.W. Streeter, A.L. Nachlas, M.E. Brown, R. Gaetani, K.L. Christman, M. E. Davis, A bioprinted cardiac patch composed of cardiac-specific extracellular matrix and progenitor cells for heart repair, Adv. Healthc. Mater. 7 (2018) 1800672.
[188] M.P. Chapman, J.L.L. Gonzalez, B.E. Goyette, K.L. Fujimoto, Z.W. Ma, W. R. Wagner, M.A. Zenati, C.N. Riviere, Application of the HeartLander crawling robot for injection of a thermally sensitive Anti-remodeling agent for myocardial infarction therapy, in: 32nd Annual International Conference of the IEEE Engineering-in-Medicine-and-Biology-Society (EMBC 10)Buenos Aires, Argentina, 2010, pp. 5428–5431.
[189] J.H. Sampson, G. Archer, C. Pedain, E. Wembacher-Schroder, M. Westphal, S. Kunwar, M.A. Vogelbaum, A. Coan, J.E. Herndon, R. Raghavan, M.L. Brady, D. A. Reardon, A.H. Friedman, H.S. Friedman, M.I. Rodriguez-Ponce, S.M. Chang, S. Mittermeyer, D. Croteau, R.K. Puri, Poor drug distribution as a possible explanation for the results of the PRECISE trial, J. Neurosurg. 113 (2010) 301–309.
[190] E. Allard, C. Passirani, J.-P. Benoit, Convection-enhanced delivery of nanocarriers for the treatment of brain tumors, Biomaterials 30 (2009) 2302–2318.
[191] Y. Mardor, O. Rahav, Y. Zauberman, Z. Lidar, A. Ocherashvilli, D. Daniels, Y. Roth, S.E. Maier, A. Orenstein, Z. Ram, Convection-enhanced drug delivery: increased efficacy and magnetic resonance image monitoring, Cancer Res. 65 (2005) 6858–6863.
[192] X. Mei, D. Zhu, J. Li, K. Huang, S. Hu, Z. Li, B.L. de Juan Abad, K. Cheng, A fluid-powered refillable origami heart pouch for minimally invasive delivery of cell therapies in rats and pigs, Med 2 (2021) 1253–1268 (e1254).
[193] S.H. Lee, Q.Q. Wan, A. Wentworth, I. Ballinger, K. Ishida, J.E. Collins, S. Tamang, H.W. Huang, C.C. Li, K. Hess, A. Lopes, A.R. Kirtane, J.S. Lee, S. Lee, W. Chen, K. Wong, G. Selsing, H. Kim, S.T. Buckley, A. Hayward, R. Langer, G. Traverso, Implantable system for chronotherapy, Sci. Adv. 7 (2021) eabj4624.
[194] J. Koo, S.B. Kim, Y.S. Choi, Z.Q. Xie, A.J. Bandodkar, J. Khalifeh, Y. Yan, H. Kim, M.K. Pezhouh, K. Doty, G. Lee, Y.Y. Chen, S.M. Lee, D. D'Andrea, K. Jung, K. Lee, K. Li, S. Jo, H.L. Wang, J.H. Kim, J. Kim, S.G. Choi, W.J. Jang, Y.S. Oh, I. Park, S. S. Kwak, J.H. Park, D. Hong, X. Feng, C.H. Lee, A. Banks, C. Leal, H.M. Lee, Y. G. Huang, C.K. Franz, W.Z. Ray, M. MacEwan, S.K. Kang, J.A. Rogers, Wirelessly controlled, bioresorbable drug delivery device with active valves that exploit electrochemically triggered crevice corrosion, Sci. Adv. 6 (2020) eabb1093.
[195] A. Ghosh, L. Li, L.Y. Xu, R.P. Dash, N. Gupta, J. Lam, Q.R. Jin, V. Akshintala, G. Pahapale, W.Q. Liu, A. Sarkar, R. Rais, D.H. Gracias, F.M. Selaru, Gastrointestinal-resident, shape-changing microdevices extend drug release in vivo, Sci. Adv. 6 (2020) eabb4133.
[196] W. Li, J. Tang, R.N. Terry, S. Li, A. Brunie, R.L. Callahan, R.K. Noel, C. A. Rodríguez, S.P. Schwendeman, M.R. Prausnitz, Long-acting reversible contraception by effervescent microneedle patch, Sci. Adv. 5 (2019) eaaw8145.
[197] C.W. Yang, T. Sheng, W.H. Hou, J. Zhang, L. Cheng, H. Wang, W. Liu, S.Q. Wang, X.M. Yu, Y.Q. Zhang, J.C. Yu, Z. Gu, Glucose-responsive microneedle patch for closed-loop dual-hormone delivery in mice and pigs, Sci. Adv. 8 (2022) eadd3197.
[198] W. Park, V.P. Nguyen, Y. Jeon, B. Kim, Y.X. Li, J. Yi, H. Kim, J.W. Leem, Y.L. Kim, D.R. Kim, Y.M. Paulus, C.H. Lee, Biodegradable silicon nanoneedles for ocular drug delivery, Sci. Adv. 8 (2022) eabn1772.
[199] J. Lee, H.R. Cho, G.D. Cha, H. Seo, S. Lee, C.K. Park, J.W. Kim, S.T. Qiao, L. Wang, D. Kang, T. Kang, T. Ichikawa, J. Kim, H. Lee, W. Lee, S. Kim, S.T. Lee, N.S. Lu, T. Hyeon, S.H. Choi, D.H. Kim, Flexible, sticky, and biodegradable wireless device for drug delivery to brain tumors, Nat. Commun. 10 (2019).